Evaluation of zwitterionic starch filler in thermoset polyurethanes on the anti-thrombogenicity activity as candidates for cardiovascular applications

Jhoan Felipe Cespedes Rojas
Chemical Engineer

Degree project submitted in compliance with the requirements for the degree of Master in Design and Management Process emphasized in Chemical Processes.

Manuel Fernando Valero Valdivieso, Dr.
Advisor

Luis Eduardo Diaz Barrera, Dr.
Said Jose Arevalo Alquichire, Dr.
Co- advisors

Universidad de La Sabana
Engineering School
Master in Design and Management Process
Chía, Colombia
2022

Dedicatory

To my grandmothers and my parents, who owing to their love, care, and teachings, I have reached these accomplishments.

Acknowledgments

I am thankful to the University of La Sabana which is my alma mater and allowed me to develop my aptitudes. Also, for the scholarship that this institution gave me to study this master's degree.

Furthermore, I want to express first my grateful gratitude to my advisor Professor Manuel Valero Valdivieso, who believed in me and develop my skills, teaching me how to aboard a problem and find a solution. Second, to Said Arevalo Alquichire because he encouraged me to follow, inspired me by his work, and his support and patience in the laboratory. Third, to Professor Luis Eduardo, for his help in the biological part of the project. Fourth, to my partners in the laboratory, especially to Rodinson Arrieta and Yomaira Uscátegui who gave me advice during the development of the research.

Finally, I thank to my friends Johan, David, Marce, and Juli who encouraged and tolerated me during difficult situations.

Prologue

This degree project was funded by Minister of Science, Technology, and Innovation of the Republic of Colombia (CT-186-2019). The exhibited work is presented as a compendium of articles (chapter 2 and 3). The products obtained from this work was:

1. Conference: “Estudio de la influencia del almidón zwitterionico sobre la propiedad antitrombogenica en poliuretanos”. Oral presentation. Simposio Argentino de Polimeros (SAP). Bahía Blanca, Argentina, 2021.

2. Published paper : Jhoan F. Cespedes, S. Arévalo-Alquichire, Luis E. Diaz., Manuel F. Valero. Influence of starch on the structure-properties relationship in polyethylene glycol/polycaprolactone diol polyurethanes. *Polymers.* 2022, 14, 3184. https://doi.org/10.3390/polym14153184.

3. Published paper: : Jhoan F. Cespedes, S. Arévalo-Alquichire, Luis E. Diaz., Manuel F. Valero. Assessment of the anti-thrombogenic activity of polyurethane starch composites. *Journal of Functional Biomaterials*. 2022, 13 (4), 184, https://doi.org/10.3390/jfb13040184

Table of Contents

Table of figures

Tables

Abstract

Cardiovascular diseases have increased worldwide due to post complications generated by SARS-Cov-2 illness, and bad food habits settled after quarantine suffered from this situation. In this context, demand for vascular grafts has increased because these devices are used to solve obstructions of blood vessels. However, the autologous graft availability is low and synthetic materials used for these cardiovascular devices have shown low thromboresistance over frame time. Polyurethanes implemented in this field have shown good mechanical properties and biocompatibility. Nevertheless, thrombogenicity activity is high yet in comparison with autologous graft. Some efforts as surface, chemical backbone modifications and inclusion of fillers in polyurethanes have shown an improvement in anti-thrombogenicity activity in the short term, but this increase in this activity did not remain over the years.

In the last years, zwitterionic moieties have been a tendency due to their anti-fouling properties, which prevent no-specific adsorption protein and the activation of cascade coagulation. These moieties have been included at the surface and inside the chemical backbone of polyurethanes. However, the inclusion of these compounds at the surface did not stay over time due to the shear force caused by blood flow. Additionally, the chemical modification of polyurethanes affects their mechanical properties to a significant degree.

Therefore, this research studied the influence of addition potato and zwitterionic starch (at 1, 2 and 3%w/w) as fillers in polyurethane matrices obtained from polycaprolactone diol (PCL), polyethylene glycol (PEG), pentaerythritol (PE), and isophorone diisocyanate (IPDI) on their physicochemical, mechanical thermal, and biological properties.Results showed that addition of potato starch (AL-N) improved tensile strength and zwitterionic starch (AL-Z) increased hydrophilicity of composites, which is a property desired in biomaterials. Also, inclusion of AL-Z reduced concentration of thrombin, protein related with clot formation. This behavior was related to the modification of chain mobility of soft domains and the interaction at the filler-polyurethane matrix at the interface.

1. Chapter 1: Overview

This chapter was made with the purpose of exposing the gap of knowledge that this research aboard through the statement of the problem and the investigations that have been made in this field, showing the breach in science that has not been considered.

1.1.Introduction

Among cardiovascular issues, Coronary Heart Disease (CHD) is the leading cause of death in the world in 2019, with a total of 9.14 million diseases, corresponding to 16.4% of the overall dies and 194 million prevalent cases for that year [1,2]. Actually, the sanitary emergency of COVID-19 that produces the Severe Acute Respiratory Syndrome (SARS-CoV-2) is expected that increase the CHD due to the virus damage to the myocardium, reinforced by the isolation caused by this virus that enlarges the poor nutrition [3,4].

CHD is defined as the obstruction of the blood vessel caused by the pile of plaques formed by cholesterol and collagen (Figure 1-1). This illness is classified as stable, unstable angina Pectoris and Myocardial infarction. These categories of CHD only are different by the severity of this obstruction, where stable angina pectoris is the least serious and myocardium infarction is the gravest condition in which the patient has the risk of loss of the myocardium [5].

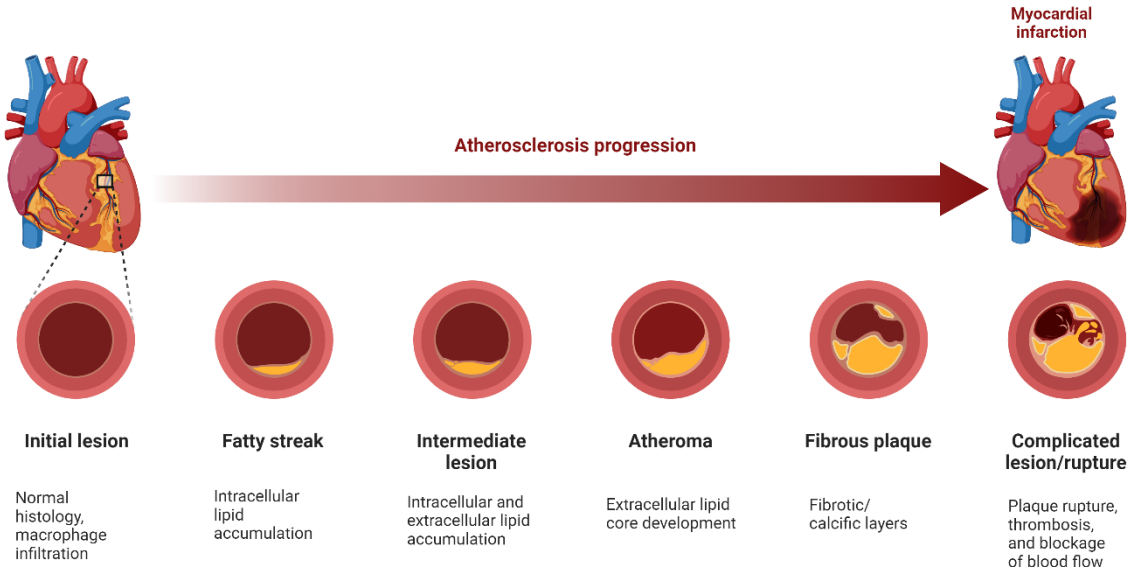

Figure 1-1. *Progress of blood vessel obstruction*

As a solution for this sickness has been implemented Coronary Artery Bypass Grafting (CABG) surgery that consists of the insertion of graft as a derivative of the blood vessel obtruded (Figure 1-2), restoring the blood flow [6]. However, the lack of autologous graft

owing to the biodisponibility of the patient, the blocking tendency of the vessel over the course of years due to the intimal hyperplasia [7], and thrombus formation inside synthetic grafts [6] make that the CABG must be done again, increasing the risk for the patient. Therefore, the antithrombogenicity activity of synthetic grafts is a property to improve the usage of these devices in the CABG, providing a solution to the lack of autologous grafts and decreasing the risk of surgery.

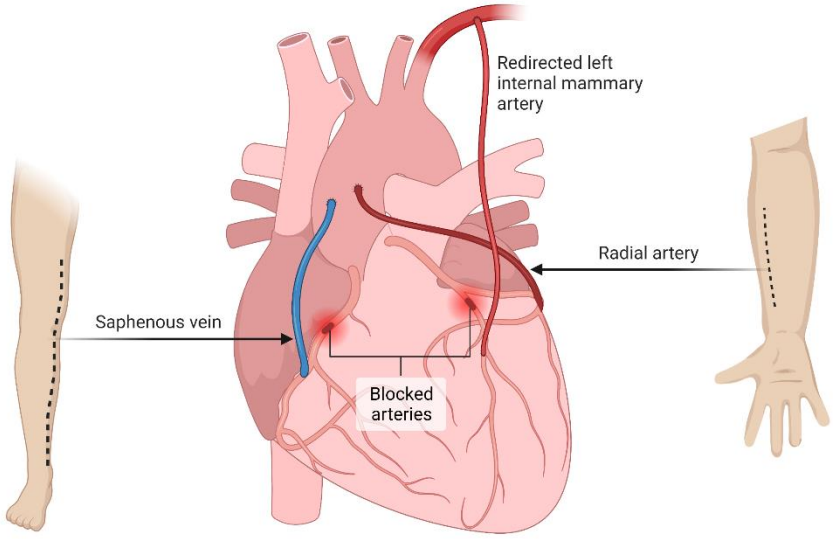

Figure 1-2. *Coronary Artery Bypass Grafting (CABG)*

Polyurethane (PU), commonly obtained by an isocyanate (C=O=N) and a polyol that can be bio-based or petrochemical [8], is used in the synthesis of diverse cardiovascular devices for its good mechanical properties analogous to the vascular tissue and biocompatibility [9,10]. Nevertheless, its antithrombogenicity activity is lower than an autologous graft, then modifications in PUs have been made to improve this activity that aboard inclusion of polysaccharides [11,12] or anticoagulant agents like heparin as a filler [13], superficial modifications [14–16] or structural chemical changes from polyol variations and the structure of isocyanate [17]. Zwitterionic compounds that are conformed by a cationic (quaternary ammonium in its majority) and anionic part (carboxybetaines, sulfobetaines and phosphorylcholine) can hydrate by dipole-dipole interactions and acquire the anti-fouling activity; therefore, its compounds are attractive to provide the antithrombogenic property to polymers used in the obtention of the synthetic graft [14,18].

Furthermore, polysaccharides that are polymers with anhydroglucose or pentoses bases (polyols) have the capacity to hydrate and confer the anti-fouling property [18]. In consequence, the inclusion of zwitterionic compounds in polysaccharides (Figure 1-3) is tendency owing to the increase of the anti-fouling property caused for its enlarged hydration ability of the compound through dipole-dipole interactions and hydrogen bonding with water molecule; also, these compounds are bio-based (provide from natural sources) and biodegradables (degrade over time) [19]. From zwitterionic polysaccharides that have been obtained, zwitterionic starch (Figure 1-3) is the more viable because it can be synthesized from a low-cost source (potato, corn, wheat, rice) and a sulfobetaine (betaine with the most feasible obtention route) [20,21].

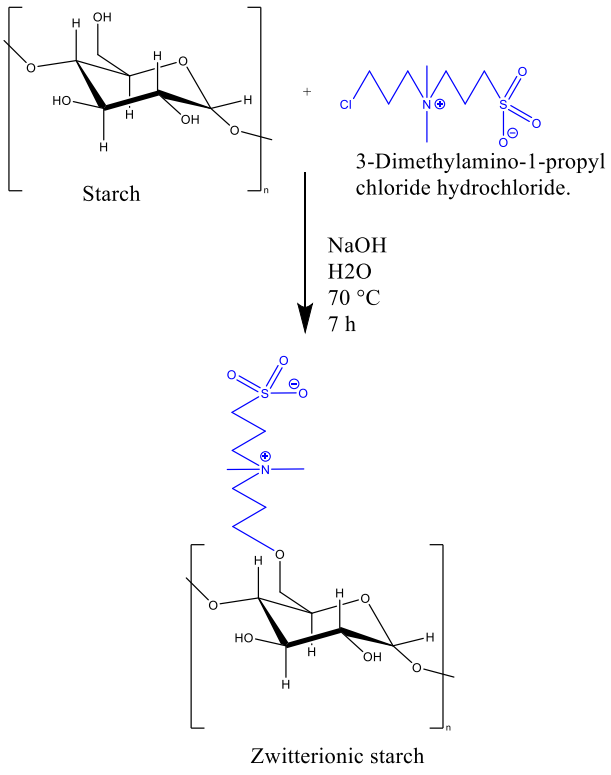

***Figure 1-3**. Synthesis of zwitterionic starch*

To the best of our knowledge, the trajectory of investigations made with biomaterials in cardiovascular applications has not been researched about the inclusion of zwitterionic

polysaccharides in polyurethanes synthesized from hydrophilic or biodegradable polyols using crosslinking agents. Therefore, this work described the relationship between physicochemical, mechanical, thermal, and anti-thrombogenic properties with the concentration of zwitterionic starch (AL-Z) as filler in polyurethanes obtained from polycaprolactone - diol (PCL), polyethylene glycol (PEG) and pentaerythritol. This relationship was characterized by FTIR, ^{1}H NMR, SEM, contact angle, swelling behavior, XRD (physicochemical properties), TGA, DSC (thermal properties), cellular viability (biocompatibility), hemolysis (hemocompatibility), platelet adhesion, protein absorption, thrombus formation, and TAT complex (anti-thrombogenicity activity). Results showed that the addition of AL-Z (compared with potato starch and polyurethane matrices) affected the physicochemical, mechanical, and biological properties in a significant matter, improving the swelling behavior and reducing the thrombus formation.

1.2. Justification

Coronary Artery Bypass Grafting (CABG) permits the restoration of the blood flow in blood vessels, avoiding the loss of myocardium [5]. Even so, in most cases, patients must wait for the availability of a graft to get the surgery, especially in Colombia, where an average of 5.2 tissues per donor is obtained, which is lower than in Europe and North America; also, Colombia has only four cardiovascular tissue banks for 50 million of residents, numbers that are low in comparison with Spain which have 23 cardiovascular tissue banks for 49 million of people, making that this country have a better infrastructure in their cardiovascular tissue banks [22]. Furthermore, the low antithrombogenicity activity of synthetic grafts increases the risk for patients in which these devices are used in CABG.

In front of this problem, several types of research have been made to improve the anti-thrombogenic property, including the inclusion of anticoagulant compounds like heparin, polysaccharides, and zwitterionic polymers on the surface of the graft or inside the biomaterial [23–27]. However, the lack of practicality in the polymers fabrication process makes them non-viable to obtain on an industrial scale; also, its intimal hyperplasia over time exhibits that anti-thrombogenic properties provided by these modifications do not endure

across time due to the erosion of the coating caused by the fluid shear stress on the material surface [28]. For this reason, the polyurethanes synthesis versatility, obtained from polyols (bio-based or biodegradables) and isocyanates, enable the PUs obtention with diverse mechanical properties to adjust to different applications, in this case, to vascular tissue [8]. Consequently, this characteristic allows the synthesis of synthetic grafts with good mechanical properties and biocompatibility; furthermore, this polymer could be complemented with the antithrombogenicity activity provided by zwitterionic compounds and polysaccharides. It shows an alternative to studying the obtention of synthetic grafts that maintain the anti-thrombogenic property over time.

Among polysaccharides, starch is the major reserve polysaccharide found in plants [29]. This fact makes that molecule attractive to the industry due to the easily available in nature and the sustainable development of products from this raw material. Additionally, it has been applied to biomedical applications for its biological compatibility and biodegradability in non-toxic compounds [30]. The use of starch as a filler in polyurethane matrices have shown an increase of polyurethane properties. Therefore, using modified starch with a zwitterion could improve the anti-thrombogenic activity of polyurethane matrix, considering that manufacturing synthetic grafts requires the antithrombogenicity, biocompatibility, and mechanical stiffness of the material [31]. Hence, it was stated the following research question:

Which is the effect of including zwitterionic starch as filler in polyurethanes obtained from PCL, PEG, and PE on the response in mechanical properties, biocompatibility, and anti-thrombogenic activity for cardiovascular applications?

1.3. State of the art

Over several years, commercial synthetic grafts like Dacron® (polyethylene terephthalate), Gore-tex® (expanded polytetrafluoroethylene), and Teflon® (polytetrafluoroethylene or PTEF) have been used owing to its high quality, losing 90% of patency over five years of usage [32]. However, these polymers used in small diameter grafts (< 6 mm) exhibit high thrombogenicity,

attributed to the loss of permeability, significant protein absorption, platelet adherence [31,33], and the lack of mechanical properties in regards to viscoelasticity and compliance [32].

Polyurethane is a common material for producing cardiovascular devices that contain hard and soft segments generated from urethane groups and crosslinkers; also, aliphatic chains of polyols that form the soft segment allow for modification of the viscoelasticity, compliance [32], high resistance, elasticity and biocompatibility [9,14]. Nevertheless, this polymer presents high thrombogenicity in comparison with autologous tissue.

In the Energy, Materials, and Environment research group (GEMA) of the University of La Sabana has been done several studies with polyurethanes were obtained from renewable resources like castor oil. Some of these investigations are related to the modification of material mechanical properties by the replacement of isocyanate group compound, changing the isophorone diisocyanate (IPDI) to diphenylmethane diisocyanate (MDI) or toluene diisocyanate (TDI), comparing the mechanical properties of these polyurethanes obtained from these diisocyanates [34] and concluding that the material stiffness increase with the enlarge crosslinking density (number of isocyanates groups per molecule) followed by the presence of the cyclic compound. Furthermore, this research group has added chitosan as a filler in polyurethanes synthesized from castor oil, reporting that this polysaccharide increases the L929 fibroblast rat cell viability in polyurethane matrices without traces of isocyanate (compound characterized as cytotoxic) [11]. Also, Arevalo., et al. [17] made a mixture design, varying polyols composition of polyethylene glycol (PEG), polycaprolactone diol (PCL), and pentaerythritol (PE) (the last one used as a crosslinker), finding that the three polyols influence the mechanical properties of PUs due to its control on phase distribution with soft and hard domains.

Other compounds that have been used as fillers in polyurethanes to improve anti-thrombogenic property are nanohydroxyapatite [35], potato starch [36], and polyhedral oligomeric silsesquioxane nano-particle (POSS (ROH)2) [37], which has reflected a slight increase in the antithrombogenicity activity. However, these compounds have affected the mechanical properties owing to a lack of interactions at the interface filler-matrix.

Also, polyurethanes have been modified in their chemical structure to enlarge antithrombotic property by the inclusion of zwitterionic compounds like the work made by Ye., et al [27], which synthesized biodegradable polyester sulfobetaine urethane ureas (PESBUUs) obtained from different concentrations polycaprolactone, making samples from 0% (conformed only by butane diisocyanate and polycaprolactone) until 100% (conformed by sulfobetaine and butane diisocyanate) and concluding that PUs with sulfobetaine reduced in a significant matter the platelet adhesion and protein absorption in comparison with polyurethanes without this compound. Moreover, it has been evidenced that the inclusion of anticoagulant agents like dipyridamole (DPA) in the chemical structure of polyurethanes with polycaprolactone and hexamethylene diisocyanate (HDI) has improved anti-thrombogenic activity [38]. However, both studies showed that the inclusion of these compounds negatively affected mechanical properties. These results were complemented with the crystallinity percentage calculated from DSC results. Reduction of mechanical properties have a direct correlation with a reduction in the percentage of crystallinity observed with the increase of sulfobetaine moiety. However, they commented that further studies with XRD should be done to define well the relation between mechanical properties and crystallinity of materials.

Surface modification is another technic used to improve the antithrombotic property in polyurethanes. Lui., et al. [23] modified the surface of polyurethanes with three different zwitterionic monomers (N,N-Dimethyl-N-(p-vinylbenzyl)-N-(3-sulfopropyl) ammonium, [2-(Methacryloyloxyethyl) ethyl]-dimethyl-(3-sulfopropyl)-ammonium and 2-Methacryloyloxyethyl phosphorylcholine). The polymerization was realized by the polyurethane surface activation with plasma at low temperature complemented with 2-Bromoisobutyryl bromide initiator. All samples were compared with polyurethanes modified with polyethylene glycol, obtaining a significant reduction in platelet adhesion and protein absorption; also, the mechanical properties of polyurethane were not affected. Additionally, between zwitterionic moieties did not have a significative difference in the antithrombotic property.

Another surface modification on polyurethanes using sulfobetaine was realized by Zhu., et al. [39], who used dopamine as a compatible compound with polyurethane due to its ability

to surface adherence as a consequence of the catechol and amine group's presence [40]. Furthermore, they formed a coordination complex with Cu^{+2} ion and dopamine free radicals, polymerizing this complex with sulfobetaine methacrylate and obtaining polyurethanes covered with methacrylates polysulfobetaine (PSBMA) and polydopamine (PDA) with Cu^{+2} ion, providing to these materials the anti-thrombogenic and antimicrobial activity.

Polysaccharides that are renewable polyols have been employed in many biomedical and technological applications as fillers in polyurethanes. Also, the zwitterionic functionalization of these polysaccharides has received great interest due to the advantage of combining biodegradability from polysaccharides and anti-fouling properties from zwitterion [18]. Zwitterionic starch is one of these polysaccharides that has been obtained by the modification of starch by sulfobetaine, showing excellent biocompatibility, high hydration, resistance to protein absorption, and stealthy behavior in front of the immune system. Zwitterionic starch, due to these properties, has been used in the fabrications of micelles for the transport of insulin and delivery of that compound in specific sites of high concentrations of glucose [19]. On the other hand, zwitterionic starch has been crosslinked with polyethylene glycol diglycidyl ether (PEGDE) and applied as anti-fouling hydrogel, exhibiting a significative reduce in platelet adhesion and protein absorption [20,41], also, this hydrogel has been utilized with dopamine to cover polytetrafluoroethylene [42]. These hydrogels did not affect the mechanical properties of materials.

From table 1 can be seen that chemical backbone modification of polyurethanes by inclusion of zwitterions and addition of fillers can improve the antithrombogenic activity of biomaterials and conserve that property for long term applications. Therefore, in this work, potato starch with a sulfobetaine moiety was include as filler in thermoset polyurethanes synthesized from PCL, PEG and PE. PEG was selected as polyol due to its high capacity to hydrate that conferred a high resistance to plasma adsorption. PCL was used to conferred biodegradability and biocompatibility to polyurethanes.

Table 1-1 State of the art of polyurethane modifications to conferred antithrombotic properties

Polyurethane modification		Mechanical properties	Thermal properties	Antithrombogenicity	Antithrombotic property durability
Chemical backbone modification	Inclusion of sulfobetaine (SB) [27].	↓	↓ Tg	↑	Large
Surface modification	Inclusion of PEG, phosphorylcholine (PC) and sulfobetaine (SB) by plasma surface treatment [23].	Not affect	Not affect	↑	Short
Addition of filler	Inclusion of nanohydroxyapatite [32], potato starch [33], and polyhedral oligomeric silsesquioxane nanoparticles [34] as filler	↓	Not reported [32,33] A slight reduction of melting point [34]	↑	Large

1.4. Objectives

1.4.1. General objective:

- To relate physicochemical, physicomechanical and antithrombotic properties of polyurethane composites with zwitterionic starch as candidates for cardiovascular applications as a function of their starch concentration.

1.4.2. Specific objectives:

- To assess physicochemical, mechanical and thermal properties of polyurethane composites synthesized from polycaprolactone diol (PCL), polyethylene glycol (PEG) and pentaerythritol (PE), using a variable concentration of zwitterionic starch as a filler.
- To evaluate the biocompatibility and antithrombogenicity activity of polyurethane composites as candidates for cardiovascular applications as a function of starch added as a filler.

1.5.References

1. Roth GA, Mensah GA, Johnson CO, Addolorato G, Ammirati E, Baddour LM, et al. Global Burden of Cardiovascular Diseases and Risk Factors, 1990–2019: Update From the GBD 2019 Study. J Am Coll Cardiol. 2020;76(25):2982–3021.

2. WHO. Mortality and global health estimates. 2020. Available from: https://www.who.int/data/gho/data/themes/mortality-and-global-health-estimates

3. Muhammad DG, Abubakar IA. COVID-19 lockdown may increase cardiovascular disease risk factors. Egypt Hear J. 2021;73(1). 10.1186/s43044-020-00127-4.

4. Zheng YY, Ma YT, Zhang JY, Xie X. COVID-19 and the cardiovascular system. Nat Rev Cardiol [Internet]. 2020;17(5):259–260.

5. Tulchinsky TH, Varavikova EA. Chapter 5 - Non-Communicable Diseases and Conditions. In: Tulchinsky TH, Varavikova EABT-TNPH (Third E, editors. San Diego: Academic Press; 2014. p. 237–309.

6. Labarrere CA, Dabiri AE, Kassab GS. Thrombogenic and Inflammatory Reactions to Biomaterials in Medical Devices. Front Bioeng Biotechnol. 2020;8. https://doi.org/10.3389/fbioe.2020.00123

7. López J, González E, Miguelena J, Martín M, Cuerpo G, Rodríguez-Roda J. Toma de decisiones en cirugía coronaria. Indicaciones y resultados del tratamiento quirúrgico del paciente con cardiopatía isquémica. Cirugía Cardiovasc. 2017;24(2):91–96.

8. Aalto-Korte K, Engfeldt M, Estlander T, Jolanki R. Polyurethane resins. In: Kanerva's Occupational Dermatology. Finnish Institute of Occupational Health, Helsinki, Finland: Springer International Publishing; 2019. p. 799–807. 10.1007/978-3-319-68617-2_53

9. Guhathakurta S, Galla S. Progress in cardiovascular biomaterials. Asian Cardiovasc Thorac Ann. 2019;27(9).744–750.

10. Navas-Gómez K, Valero MF. Why polyurethanes have been used in the manufacture and design of cardiovascular devices: A systematic review. Materials (Basel). 2020;13(15). 10.3390/ma13153250

11. Arévalo FR, Osorio SA, Valcárcel NA, Ibarra JC, Valero MF. Characterization and in vitro biocompatibility of binary mixtures of chitosan and polyurethanes synthesized from chemically modified castor oil, as materials for medical use. Polym from Renew Resour. 2018;9(1):23–38.

12. Arévalo F, Uscategui YL, Diaz L, Cobo M, Valero MF. Effect of the incorporation of chitosan on the physico-chemical, mechanical properties and biological activity on a mixture of polycaprolactone and polyurethanes obtained from castor oil. J Biomater Appl. 2016;31(5):708–720.

13. Jin Y, Zhu Z, Liang L, Lan K, Zheng Q, Wang Y, et al. A facile heparin/carboxymethyl chitosan coating mediated by polydopamine on implants for hemocompatibility and antibacterial properties. Appl Surf Sci . 2020;528:146539.

14. Adipurnama I, Yang M-C, Ciach T, Butruk-Raszeja B. Surface modification and endothelialization of polyurethane for vascular tissue engineering applications: A review. Biomater Sci. 2017;5(1):22–37.

15. Cortella LRX, Cestari IA, Guenther D, Lasagni AF, Cestari IN. Endothelial cell responses to castor oil-based polyurethane substrates functionalized by direct laser ablation. Biomed Mater. 2017;12(6). 10.1088/1748-605X/aa8353

16. Major R, Plutecka H, Gruszczynska A, Lackner JM, Major B. Effects of the surface modification of polyurethane substrates on genotoxicity and blood activation processes. Mater Sci Eng C. 2017;79:756–762.

17. Arévalo-Alquichire S, Morales-Gonzalez M, Diaz LE, Valero MF. Surface response methodology-based mixture design to study the influence of polyol blend composition on polyurethanes' properties. Molecules. 2018;23(8). 1942.

18. Erathodiyil N, Chan H-M, Wu H, Ying JY. Zwitterionic polymers and hydrogels for

antibiofouling applications in implantable devices. Mater Today. 2020;38:84–98.

19. Wen N, Lü S, Gao C, Xu X, Bai X, Wu C, et al. Glucose-responsive zwitterionic dialdehyde starch-based micelles with potential anti-phagocytic behavior for insulin delivery. Chem Eng J. 2018;335:52–62.

20. Wang J, Sun H, Li J, Dong D, Zhang Y, Yao F. Ionic starch-based hydrogels for the prevention of nonspecific protein adsorption. Carbohydr Polym. 2015;117:384–391.

21. Wang J, Li J, Yang H, Zhu C, Yang J, Yao F. Preparation and characterization of protein resistant zwitterionic starches: The effect of substitution degrees. Starch/Staerke. 2015;67(11–12):920–929.

22. Montaña Chaparro WF, Díaz Roa KA, Otálvaro Cifuentes EH. Situación actual de los bancos de tejidos en Colombia: tejido cardiovascular. Rev Colomb Cardiol . 2020;27(5):461–468.

23. Liu P, Huang T, Liu P, Shi S, Chen Q, Li L, et al. Zwitterionic modification of polyurethane membranes for enhancing the anti-fouling property. J Colloid Interface Sci. 2016;480:91–101.

24. Ma X, Sheu M, Eramo L, Wainwright J, Li J. Anti-thrombogenic medical devices and methods. 2015.

25. Wu J, Lin W, Wang Z, Chen S, Chang Y. Investigation of the Hydration of Nonfouling Material Poly(sulfobetaine methacrylate) by Low-Field Nuclear Magnetic Resonance. Langmuir. 2012;28(19):7436–7441.

26. Xiao X, Chen H, Chen S. New zwitterionic polyurethanes containing pendant carboxyl-pyridinium with shape memory, shape reconfiguration, and self-healing properties. Polymer (Guildf). 2019;180:121727.

27. Ye SH, Hong Y, Sakaguchi H, Shankarraman V, Luketich SK, DAmore A, et al. Nonthrombogenic, biodegradable elastomeric polyurethanes with variable sulfobetaine content. ACS Appl Mater Interfaces. 2014;6(24):22796–22806.

28. Belanger A, Decarmine A, Jiang S, Cook K, Amoako KA. Evaluating the Effect of Shear Stress on Graft-To Zwitterionic Polycarboxybetaine Coating Stability Using a Flow Cell. Langmuir. 2019;35(5):1984–1988.

29. Averous L, Halley PJ. Chapter 1: Starch Polymers: From the Field to Industrial Products. Starch Polym From Genet Eng to Green Appl. 2014;3–10.

30. Solanki A, Das M, Thakore S. A review on carbohydrate embedded polyurethanes: An emerging area in the scope of biomedical applications. Carbohydr Polym . 2018;181:1003–1016.

31. Heydrick S, Roberts E, Kim J, Emani S, Wong JY. Pediatric cardiovascular grafts: historical perspective and future directions. Curr Opin Biotechnol. 2016;40:119–124.

32. Faturechi R, Hashemi A, Abolfathi N, Solouk A, Seifalian A. Fabrications of small diameter compliance bypass conduit using electrospinning of clinical grade polyurethane. Vascular. 2019;27(6):636–647.

33. Vellayappan MV, Balaji A, Subramanian AP, John AA, Jaganathan SK, Murugesan S, et al. Multifaceted prospects of nanocomposites for cardiovascular grafts and stents. Int J Nanomedicine. 2015;10:2785–2803.

34. Valero MF, Díaz LE. Polyurethane networks from pentaerythritol-modified castor oil and lysine polyisocyanates: synthesis, mechanical, and thermal properties and in vitro degradation. Quim Nova. 2014;37(9):1441–1445.

35. Selvakumar M, Jaganathan SK, Nando GB, Chattopadhyay S. Synthesis and characterization of novel polycarbonate based polyurethane/polymer wrapped hydroxyapatite nanocomposites: Mechanical properties, osteoconductivity and biocompatibility. J Biomed Nanotechnol. 2015;11(2):291–305.

36. Kendaganna Swamy BK, Siddaramaiah. Structure-property relationship of starch-filled chain-extended polyurethanes. J Appl Polym Sci. 2003;90(11):2945–2954.

37. Zaredar Z, Askari F, Shokrolahi P. Polyurethane synthesis for vascular application.

Prog Biomater. 2018;7(4):269–278.

38. Xu C, Kuriakose AE, Truong D, Punnakitikashem P, Nguyen KT, Hong Y. Enhancing anti-thrombogenicity of biodegradable polyurethanes through drug molecule incorporation. J Mater Chem B. 2018;6(44):7288–7297.

39. Zhu Z, Gao Q, Long Z, Huo Q, Ge Y, Vianney N, et al. Polydopamine/poly(sulfobetaine methacrylate) Co-deposition coatings triggered by CuSO4/H2O2 on implants for improved surface hemocompatibility and antibacterial activity. Bioact Mater. 2021;6(8):2546–2556.

40. Lee H, Dellatore SM, Miller WM, Messersmith PB. Mussel-Inspired Surface Chemistry for Multifunctional Coatings. Science (80-). 2007;318(5849):426 LP – 430.

41. Wang J, Li J, Yang H, Zhu C, Yang J, Yao F. Preparation and characterization of protein resistant zwitterionic starches : The effect of substitution degrees. 2015;1–10.

42. Yao M, Sun H, Guo Z, Sun X, Yu Q, Wu X, et al. A starch-based zwitterionic hydrogel coating for blood-contacting devices with durability and bio-functionality. Chem Eng J. 2021;421:129702.

2. Chapter 2. Influence of starch on the structure-properties relationship in polyethylene glycol/polycaprolactone diol polyurethanes

The reader in this chapter will find the physicochemical, mechanical, and thermal characterization of polyurethanes composites made from polyurethane matrices with the addition of potato (AL-N) and zwitterionic starches (AL-Z). The characterization of the effect of this inclusion was made by attenuated total reflectance-fourier transform infrared spectroscopy (ATR-FTIR), contact angle, swelling behavior, thermogravimetric analysis (TGA), tensile/strain, scanning electron microscope (SEM), dynamic mechanic analysis (DMA), differential scanning calorimetry (DSC) and X-ray diffraction (XRD). The results showed that AL-N and AL-Z modified these properties, where AL-N improved tensile strength in 30%, and AL-Z increased the hydrophilicity of polyurethanes (PUs) matrices in 53%; additionally, AL-N had interactions with the soft segments and AL-Z had interactions with the hard segments according to ATR-FTIR results. Finally, both fillers reduced the degree of crystallinity and did not affect the thermal stability of polyurethanes due to the disruption of hydrogen bonding between N-H, C-O-C and C=O groups.

2.1. Introduction

Composite polymers tend to be used in cardiovascular applications [1] due to their versatility in terms of their mechanical, thermal, and physicochemical properties, which are achieved by mixing a disperse phase (filler) and a continuous phase (polymeric matrix) [1,2]. Several investigations with different polymeric matrices have been conducted to obtain new composite materials for cardiovascular implants, especially with alginate, poly(D,L-lactic-co-glycolic acid) (PLGA), polytetrafluoroethylene (PTEF), polyethylene terephthalate (Dacron) and polyurethane (PU) [3–8]. Between these polymeric matrices, polyurethanes are listed as the first candidate for the production of vascular grafts owing to their better compliance, biocompatibility, mechanical properties, and adaptation to different manufacturing technologies [9,10].

Polyurethane is a group of polymers synthesized by a polycondensation reaction between an isocyanate and polyol [11]. During polycondensation, urethane groups are formed and begin to interact with polar groups present in polyols. As a consequence, a hard crystalline domain appears that is held together due to hydrogen bonding. In contrast, interactions between the polyols are weak, and a soft domain is produced [9,12]. The mechanical properties of polyurethane can be modified by the change of soft and hard segments controlling the flexibility and hardness of the polymer. Thus, graft compliance can be optimized by varying concentrations of those segments [12]. Polyester and polyether blends have been studied to improve the biological and mechanical performance of polyurethanes. In fact, polycaprolactone-diol (PCL) has shown promising results referred to as biocompatibility and mechanical properties. It is associated with the interactions of hard segments. Moreover, polyethylene glycol (PEG) is often used to provide flexibility and antithrombogenicity activity [12,13]. Despite this, blends of these polyols have been used in the synthesis of polyurethane for biomedical applications [14,15]. Recently, investigations have shown that the inclusion of fillers in polymeric matrices constituted by different polyols can improve mechanical and thermal properties [16,17].

Certain studies have reported the improvement in the mechanical properties of polyurethane with the addition of natural fillers such as nanoparticles of chitosan, cellulose, and starch. Villani M., et al. [18] studied the effect of loading TiO_2, chitosan and silver in polyurethane, finding that chitosan and silver could be used as fillers for medical applications. Another investigation conducted by Arevalo F. R., et al. [19] concluded that adding chitosan as a filler in a polyurethane matrix synthesized from castor oil does not affect mechanical and thermal properties but also improves the L929 cell's viability. Furthermore, Hormaiztegui M., et al. [20] added cellulose nanocrystals to the polyurethane matrix, finding that the mechanical and thermal properties were reinforced. Around starch particles, Gaaz T., et al. [21] loaded starch in a thermo-plastic polyurethane matrix, reporting that fillers increase tensile strength by 17% with 1.5% starch.

Starch has been widely used in biomaterials and has potential applications, especially in cell seeding, tissue engineering and implants for bone replacement [22]. This polysaccharide composed of amylose and amylopectin [22,23] is the second largest natural polymer found in plants as granules after cellulose, making it an extensive source of low-cost polymers. Polysaccharide is attractive for biomaterial due to its properties such as its biodegradability and because its degradations products are non-toxic; additional benefits include its biocompatibility, hydrophilicity, high chemical reactivity and polyfunctionality [24,25]. However, starch has poor mechanical strength, causing it to need to be modified chemically or blended with other polymers [24].

One modification that can make starch a better material for cardiovascular applications is the inclusion of a zwitterionic moiety. Zwitterions are molecules that have mixed charge pairs, which confer super hydrophilicity and non-fouling properties [26]. Using a Williamson etherification reaction, Wang., et al. [27] obtained zwitterionic starch from sulfobetaine and potato starch, which include the zwitterion moiety in the anhydroglucose unit and characterized the protein adsorption, cytotoxicity, and cell adhesion. They concluded that starch-modified material has protein adsorption resistance, good biocompatibility and can resist cell adhesion.

From the trajectory of studies in the cardiovascular applications of composites polyurethanes to the best of our knowledge, investigations have not been carried out on the relationship between starch (natural and modified with sulfobetaine) and soft and hard segments in polyurethane matrices, aside from its influence on mechanical and thermal properties. Therefore, this work describes the relationship between the concentrations of starch in polyurethane matrices synthesized from polycaprolactone diol (PCL), polyethylene glycol (PEG), and pentaerythritol (PE), with different soft and hard segments on physicochemical, mechanical, and thermal properties and the inter-actions of starch with those segments. We find that the interaction of starch with polyurethane matrices depends on its functional groups. Moreover, these interactions modify the mechanical and physicochemical properties to a significant degree.

2.2. Materials and methodology

2.2.1. Materials

Polycaprolactone diol (PCL-diol, Mw~2000), isophorone diisocyanate (IPDI), potato starch (soluble), N,N-Dimetylformamide (anhydrous, 99.8%) (DMF), 1,3-Propanesultone (PS) (98%), 3-Dimethylamino-1-propyl chloride hydrochloride (96%) (CDMAP*HCl) and dichloromethane (anhydrous, ≥ 99.8%) were supplied by Sigma-Aldrich (St. Louis, MO, USA). Polyethylene glycol (PEG, Mw~1000) and Sodium hydroxide were provided by Merck KGaA (Darmstadt, Germany). Pentaerythritol (PE) was obtained from Alfa Aesar (Heysham, UK) and Acetic acid glacial (99.7%) from Central Drug House (P) Ltd. (Vardaan House Ansari Road, Daryaganj, New Delhi, India).

2.2.2. Methodology

2.2.2.1. Synthesis of Zwitterionic starch

The obtention of zwitterionic starch was carried out using Williamson etherification. Briefly, 4.02 M CDMAP*HCl in distilled water was neutralized with the addition of 40% NaOH (keeping the stoichiometry relationship) and the oil phase (CDMAP) was decanted. In addition, CDMAP was added to PS (1.36 M in dichloromethane), reacting for 24 h at 28 ± 2 °C in a nitrogen atmosphere. The product that was precipitated (3-dimethyl(chloropropyl)

ammonium propanesulfonate or DCAPS) was washed three times with dichloromethane, dried and stored under vacuum, and its obtention was confirmed by ^{1}H NMR [27]. Moreover, potato starch was activated with 25% NaOH, keeping the mol relationship of the NaOH/anhydroglucose unit at 1:2.5. DCAPS (2.46 M in distilled water), which reacted with the activated potato starch (2.19 M in water distilled) at 55 ± 2 °C for 12 h. The product in the solution reaction was neutralized with acetic acid glacial at a pH of 7 and precipitated with methanol, and we washed the solution reaction three times (Figure A **1**) [27,28]. The size of zwitterionic starch was reduced by pulverizing it in a mortar and sieving it in a 90 µm mesh.

2.2.2.2. Chemical structure, thermal and morphology characterization of zwitterionic starch

The obtention of zwitterionic starch was evaluated by Fourier transform infrared spectroscopy using diamond attenuated total reflection (ATR-FTIR) and Proton Nuclear Magnetic resonance (^{1}H NMR). ATR-FITR was taken with a Cary 630 FTIR spectrometer (Agilent, Santa Clara, CA, USA), recording in a range of 650 cm^{-1} to 4000 cm^{-1} with an average of eight scans and a resolution of 2 cm-1. 1H NMR was measured with a Bruker Avance III spectrometer of 400 MHz (Billerica, Massachusetts, USA), using 32 scans and D_2O as solvent at 25 °C. The degree of substitution was obtained from equation 1, using 1H NMR integrals data from the peaks "c"(∫c) and "C1" (∫C1) corresponding to the resonance of hydrogens (which each methyl group contain 3 hydrogens) of the quaternary ammonium group in the sulfobetaine moiety and carbon 1 in the anhydroglucose unit [27,28].

$$DS=\int c/(\int C1*6) \quad (1)$$

Thermal characterization was carried out by Thermogravimetric Analyses (TGA) and Differential Scanning Calorimetry (DSC). TGA measured the thermal stability of zwitterionic starch in two steps under a nitrogen atmosphere (100 mL/min) using a TGA/DSC 1 (Mettler Toledo, Columbus, OH, USA). First, water from modified starch was removed at 106 °C for 1 h. Then, samples were heated at 10 °C/min until 600 °C. DSC was taken with DSC 3+ (Mettler Toledo, Columbus, OH, USA), using a nitrogen atmosphere (100 mL/min) in a range of -70 °C to 150 °C with a ramp of 5 °C/min [29].

The surface morphology of zwitterionic starch was studied by Scanning Electron Microscopy (SEM), using a TESCAN LYRA3 (Brno, Czech Republic) and each sample where gold plated[30].

2.2.2.3. Synthesis of composites polyurethanes

Polyurethanes were synthesized by the prepolymer method [31]. First, melted polyols (PEG and PCL) at 110 °C reacted with IPDI at 70 °C and 300 rpm for 15 min, obtaining a prepolymer. Second, a solution of PE 0.497 M in DMF at 110 °C was made, and we added that solution to the prepolymer and carried out the experiment at 70 °C and 300 rpm for 15 min, keeping a mol relationship of 1:1 NCO/mol OH [12,31]. The addition of starch (native and zwitterionic) was made after crosslinking with PE and homogenizing the powder in the media at 70 °C and 300 rpm for 15 min [31]. Films of composite polyurethanes were obtained when the composite was poured into a stain-less steel mold and cured at 110 °C for 12 h [32]. The composition in the weight of polyols and starch (native and zwitterionic) are exhibited in Table 1, where composition P1 correspond to 5% PEG – 90% PCL – 5% PE, composition P2 corresponds to 45% PEG – 45% PCL – 10% PE and composition P3 corresponds to 46.25% PEG – 46.25% PCL – 7.5% PE. Our laboratory previously studied the biological performance of PEG-PCL-PE polyurethanes and based on that work we selected the compositions with the best biological results.

***Table 2-1**. Samples of composites PU*

PEG	PCL	PE	Starch	Sample*
5%	90%	5%	0%	P1-0%-AL
			1%	P1-1%-AL-(N ó Z)
			2%	P1-2%-AL-(N ó Z)
			3%	P1-3%-AL-(N ó Z)
45%	45%	10%	0%	P2-0%-AL
			1%	P2-1%-AL-(N ó Z)
			2%	P2-2%-AL-(N ó Z)
			3%	P2-3%-AL-(N ó Z)
46.25%	46.25%	7.5%	0%	P3-0%-AL
			1%	P3-1%-AL-(N ó Z)
			2%	P3-2%-AL-(N ó Z)
			3%	P3-3%-AL-(N ó Z)

* "AL" refers to starch (native and zwitterionic). "N" makes allusion to native starch and "Z" refers to zwitterionic starch.

2.2.2.4. Physicochemical characterization

Composite polyurethane chemistry was described by ATR-FTIR with the Cary 630 FTIR spectrometer (Agilent, Santa Clara, CA, USA) in a range of 650 cm^{-1} to 4000 cm^{-1} [30]. Water absorption was studied by the weight of the material before (W0) and after soaking in distilled water (WSx) at different times. Four points on the first day and three points per day in the next three days were recorded [32,33]. Equation 2 was used to determine the percentage of water absorption. The contact angle was measured by the sessile drop method, using the equipment MobileDrop (gh11, Krüss, Germany) and distilled water at 20 °C as a test liquid. The average measurement of the contact angle corresponds to ten values of each polymeric material [33,34].

$$\% \text{ Water absorption} = ((WSx - W0)/W0) * 100\% \quad (2)$$

2.2.2.5. Thermo-mechanical properties

The tensile/strain test was performed according to ASTM D638-1 in an EZ-LX (SHIMADZU, Kioto, Japan) with a 5kN load cell and a deformation rate of 10 mm/min. This test was conducted in triplicate and each sample had dimensions of 40 x 6 x 3 mm (length x width x thickness) [34]. The morphologies of the interphase between fillers and polymeric matrices were studied by SEM in a TESCAN LYRA3 (Brno, Czech Re-public) [30,35].

The storage modulus and the loss factor were evaluated by dynamic mechanical analysis (DMA) in a DMA 850 (TA Instruments, New Castle, Delaware, USA) with a frequency of 1 Hz and a deformation of 1 mm with a force of tension. Samples of 20 mm x 5 mm x 1.5 mm (length x width x thickness) were heated with a ramp of 5 °C/min between -70 °C and 120 °C [31].

X-Ray diffraction (XRD) was measured in a X´PERT PRO MPD (PANalytical, Malvern, Worcestershire, United Kingdom) with a Cu α radiation at 45 kV and 1.54 Å. The measurement range was between 5 – 70 ° (2theta). Equation 3 was used to calculate the degree of crystallinity (DC) of composite materials, using integrals of XRD curves, where (Ic) is the area under the crystalline peak and (Ia) is the amorphous area [36].

$$DC = (Ic/(Ic + Ia)) * 100\% \quad (3)$$

Thermal transitions and thermal stability were studied by DSC and TGA. DSC was measured in a DSC3+ (Mettler Toledo, Columbus, OH, USA) under a nitrogen atmosphere (100 mL/min) between the range of -70 °C to 150 °C with a ramp of 5 °C/min. TGA was evaluated in a TGA/DSC (Mettler Toledo, Columbus, OH, USA) in two steps under a nitrogen atmosphere (100 mL/min). First, samples were exposed to an isothermal step at 106 °C for 1 h. Then, samples were heated at 10 °C/min in the range of 106 °C to 600 °C [12].

2.2.2.6. Statistics analysis

Experiments were carried out using three independent replicates. The results are presented as a mean value ± standard deviation (SD). Data were analyzed by ANOVA of two factors to study the effect of the starch type (factor 1) and its concentration (factor 2) inside the PU matrix. Additionally, PU matrices without fillers was evaluated via ANOVA of one-way. The assumptions of normality, homoscedasticity, and in-dependence were validated. Significant differences were found by a Tukey test. A P-value of less than or equal to 0.05 was considered significant.

2.3. Results and discussion

The obtention of the zwitterionic molecule (DCAPs) was confirmed by ^{1}H RMN. Figure A 2 shows the ^{1}H RMN spectrum, in which five peaks were identified. Peak c (δ=3.01) has the major intensity due to it having a higher number of hydrogens (6 H) with the same resonance than other groups in the molecule. These hydrogens are in the same electronic environment, near nitrogen with a positive charge (quaternary ammonium). The resonance of hydrogens near of sulfonate group corresponds to peak d (δ=2.86). Additionally, peaks c and d appeared in the ^{1}H RMN spectrum of zwitterionic starch (AL-Z) shown in Figure 2-1A, proving the modification of potato starch (AL-N) with the zwitterion (DCAPs). Another technique used to support the modification of starch was ATR-FITR. Comparing FTIR spectra of AL-N and AL-Z shown in Figure A **3**, two new bands were identified in AL-Z FTIR spectrum. These two new bands at 1481 cm^{-1} and 1202 cm^{-1} exhibited in Figure 2-1B, are attributed to N-C and S=O stretching, confirming the inclusion of zwitterionic moiety in anhydroglucose unit of starch. These results are consistent with Wang., et al. [27], who first synthesize DCAPs

and then zwitterionic starch. DCAPs was used to modify potato starch by Williamson etherification. ^{1}H RMN and FTIR spectra confirmed both products.

The degree of substitution (DS) defined as the average number of hydroxyl groups substituted per anhydroglucose unit [37], was estimated with equation 1 to find the inclusion of the zwitterionic moiety in potato starch. This value could vary in the range of 3 to 0, where 3 is the maximum and 0 is the minimum of zwitterion in starch. The areas of peaks c and C1 (hydrogen attached to carbon 1 in the anhydroglucose unit) of four replicas of synthesis (Figure A 4) were used to calculate the DS, the value of which was 0.547 ± 0.03. This result is similar to the maximum DS of 0.46 obtained by Wang., et al. [28], who studied the degree of substitution of the zwitterion moiety on potato starch at different temperatures, solvents, and mol relationships of NaOH and DCAPS with anhydroglucose unit.

The thermal stability of starches (AL-N and AL-Z) was measured by TGA. Thermograms (Figure A 5) show the weight loss percentage of samples with the increment in temperature. The degradation steps of AL-N, DCAPS and AL-Z were exposed in the derivative thermogram (DTG) exhibited in Figure 2-1C. All samples have two steps of degradation, where AL-N presents the first step between 218 °C – 341 °C, which is related to the main degradation (pyrolysis) of amylose and amylopectin, and the second step in the range of 341 °C to 600 °C is attributed to the formation of carbon black [29,38]. The DTG of DCAPS shows the first step of degradation between 210 °C – 308 °C, which is assigned to a Hoffman elimination of the qua-ternary ammonium [39] and the degradation of the sulfonate group. Additionally, the second step around 410 °C could be due to the breakup of the carbon chain [40]. AL-Z presented two steps of degradation, similar to AL-N and DCAPS, where the first step in the range of 220 °C – 330 °C is associated with the degradation of the main chains (amylose and amylopectin) of starch-modified and the second steps around 600 °C are related to the formation of carbon black. In the degradation steps of AL-Z, especially in the first step, there is an overlap between the degradation of the quaternary ammonium and sulfonate group with the break-up of amylose and amylopectin chains. Additionally, at the end of the first step of the degradation of AL-N, AL-Z lost less mass (15%) in comparison with AL-N, which lost

35% of its mass. This phenomenon is associated with an improvement in thermal stability due to the inclusion of sulfonate groups [41,42].

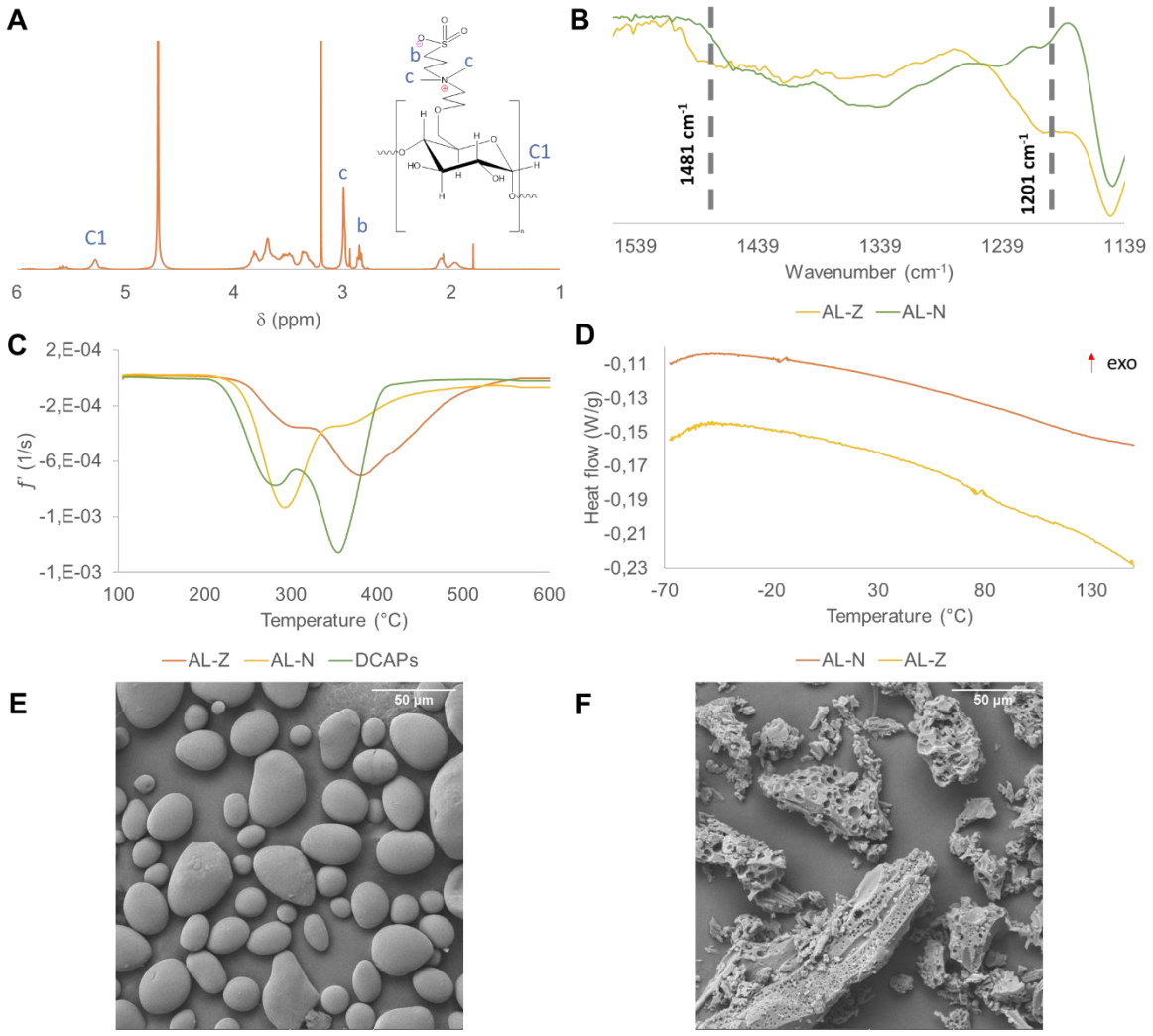

Figure 2-1. *Characterization of starch (zwitterionic and native) by (A) 1H RMH, (B) ATR-FTIR, (C) DTG, (D) DSC, and SEM of (E) potato starch and (F) zwitterionic starch*

The thermal transitions of starches were studied by DSC. AL-N and AL-Z did not present any thermal transition (Figure 2-1D). Some investigations [43–46] have reported thermograms of potato starch, which presented a peak between 80 °C – 110 °C related to gelatinization, a phenomenon that refers to a loss of structural order in amylopectin and amylose chains, depending on the content of moisture. Therefore, the peak absence in AL-Z

and AL-N in Figure 2-1D after 80 °C indicated that samples do not present moisture and are thermally stable, principally AL-Z.

Images obtained by SEM showed that potato starch (Figure 2-1E) has a spherical shape and smooth surface with 24.4 ± 7.5 µm (n=10) particle size. In contrast, AL-Z (Figure 2-1F) exhibited a porous surface and a non-uniform shape with a particle size of 88.5 ± 14.3 µm (n=10), which is greater than AL-N. This change in the AL-Z morphology could be due to the reduction of hydroxyl number with the inclusion of the zwitterion moiety and the rupture of hydrogen bonding in the polysaccharide.

After obtention of AL-Z, polyurethane composites were synthesized and evaluated by ATR-FTIR. Figure 2-2 shows FTIR spectra of polyurethanes P1, P2 and P3 without fillers, where FTIR bands in 3350 cm-1 (N-H stretching), 1725 cm^{-1} (C=O stretching) and 1531 cm^{-1} (N-H flexion) confirmed the obtention of polyurethanes. The presence of PCL and PEG segments in polyurethanes was observed in FTIR spectrums, in which the ester group of PCL is related to peaks at 1229 cm^{-1} (C-C(O)-O asymmetric stretching), and the increase in the intensity of the band at 1725 cm^{-1} (only in P1); moreover, the ether group is assigned to the band at 1162 cm^{-1} (C-C-O asymmetric stretching) [19,30]. The absence of the 2225 cm^{-1} peak assigned to the isocyanate group suggests that the IPDI completely reacted; that must be ensured due to the cytotoxic effect of that compound [31]. Finally, S. Arevalo-Alquichire., et al. [12] acquired similar results for polyol compositions similar to the ones used in this study.

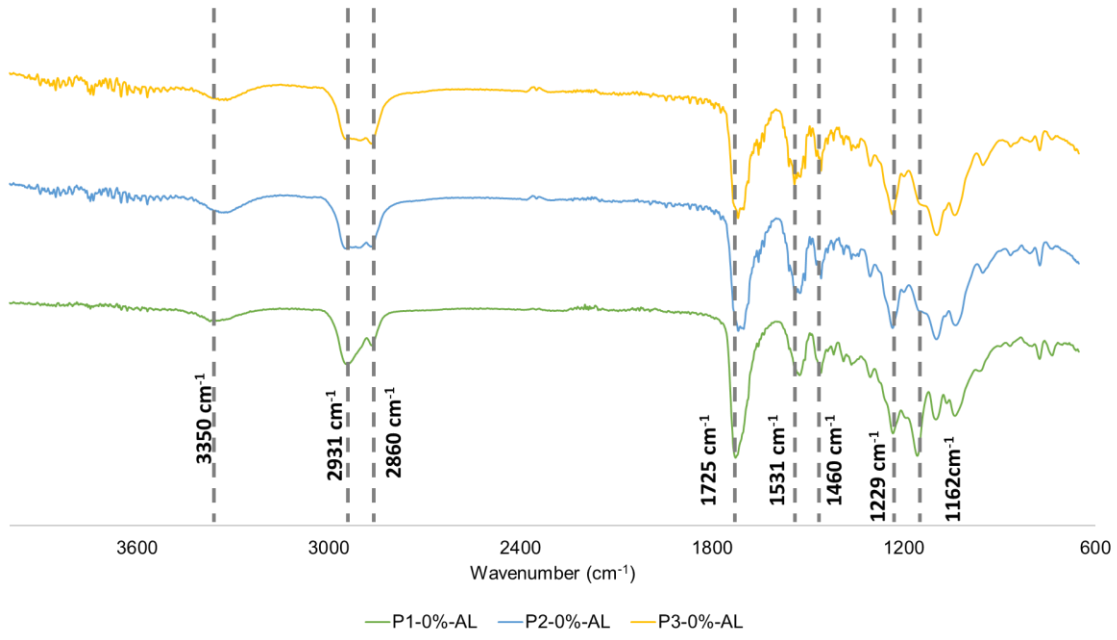

Figure 2-2. *FTIR spectrum of polyurethane matrices.*

The FTIR spectrum of composites polyurethanes is shown in Figure A **6**. Intermolecular interactions between fillers and hard and soft segments of polyurethane matrices at the interface were evaluated by peaks at 3350 cm^{-1}, 3325 cm^{-1}, 1723 cm^{-1}, 1700 cm^{-1}, 1097 cm^{-1} and 1039 cm^{-1} (Figure 2-3). From Figure 2-3A, it could be seen that polymeric matrices P2 and P3 showed a displacement to the right side (3325 cm^{-1}) in comparison with the peak for P1 (3350 cm^{-1}). This phenomenon could be explained by the growth of hydrogen bonding between N-H (urethane group) and C-O-O (Ether group)[47–49]. Furthermore, the intensity for this band in P2 increased in comparison to P1 and P3, which indicated an enlarged concentration of urethane groups [31]. These facts permit us to infer that the concentration of crosslinker in polymeric matrix controls the number of urethane groups and the interactions in hard domains [31,47,49]. This statement is complemented with the behavior in Figure 2-3B and Figure 2-3C, where a peak appears at 1700 cm^{-1} and increases the intensity at 1039 cm^{-1}; it is related to the stretching of C=O (ester group) and C-O-C (ether group) with hydrogen bonding [48,50]. These results are consistent with Wongsamut., et al. [47], who made Polycarbonate-based thermoplastic polyurethane elastomers and studied the content of

hard segments. They found that high concentrations of hard domains increase the number of hydrogen bondings.

Figure 2-3D - Figure 2-3F exhibit a disruption at 1039 cm^{-1} for P1-3%-AL-N in comparison with P1-0%-AL. That band is related to the stretching of C-O-C of the ether group; thus, the enlargement of this band could be explained by the disturbance of hydrogen bonding between urethane groups and ether groups of polyethylene glycol [51], caused for the inclusion of potato starch at this concentration. Similar results were obtained by Malay O,. et al. [51], who made composites from silica nanoparticles and thermoplastic polyurethane urea (TPU), concluding that silica nanoparticles interact more strongly with soft segments than with hard domains.

Furthermore, the decrease of the 3350 cm^{-1} peak intensity with the increment of AL-Z concentration in P1 matrix polyurethane (Figure 2-3G) could be assigned to a reduction of hydrogen bonds between N-H and C=O groups [49,52]. These results are consistent with the investigation conducted by Lee, H.S., et al. [52], who studied the phase separation rate between soft and hard segments of polyurethanes at different temperatures, finding that an increase in peak intensity of 3330 cm^{-1} is related to an enlarged number of hydrogen bonds between N-H and C=O groups, and it indicated that hard and soft segment phase separations increased. From Figure 2-3H and Figure **2-3**I, AL-Z filler did not affect the hydrogen bonds between groups of hard domains in P2 and P3 polyurethane matrices.

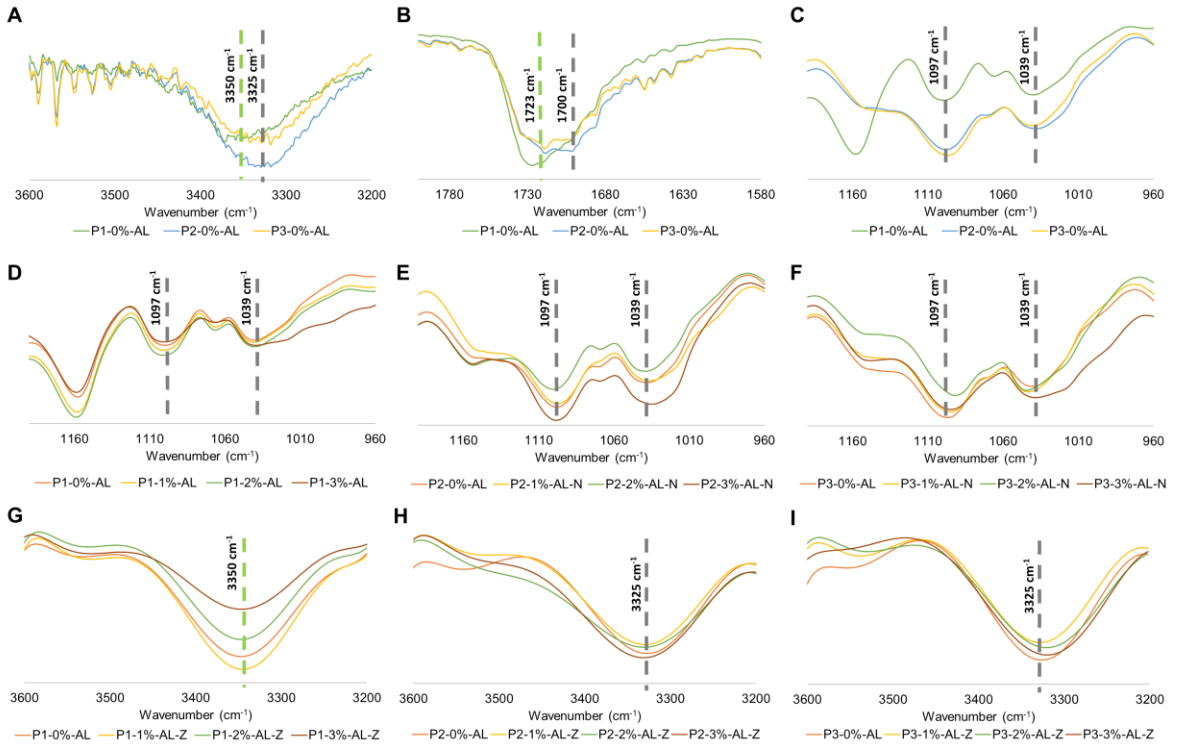

***Figure 2-3**. FTIR regions of PUs matrices (A)-(C) without filler, (D)-(F) with AL-N in C-O-C region and (G)-(I) with AL-Z in N-H region.*

The surface hydrophilicity of composites polyurethanes was evaluated using the contact angle (Table 2-2). Polymeric matrices without filler did not have any significant change in their contact angle. However, other studies that included PEG in the polyurethane backbone [53–55] observed that a major concentration of this polyol reduces the contact angle value and then shows enlarged hydrophilicity. This tendency could be explained by the increase in the soft segment backbone polyurethane chains' mobility, where polar groups (especially PEG) can migrate to the surface and reduce the interfacial energy [55]. Therefore, it could be inferred that the concentration of PEG in our polyurethane formulations was not significant enough to enlarge the mobility of chains in soft segments.

***Table 2-2**. Contact angle, water absorption, thermal degradation, and mechanical properties of composite PUs*

PU	Starch	Concentration	Contact angle (°)**	Area under curve (%Wt*h)**	Tmax (°C)**	Tensile strenght (σ) (MPa)**	Module (E) (MPa)**
P1		AL-0%	103.7 ± 6.6^{a}	1.60 ± 0.93^{a}	420.29 ± 12.61^{a}	2.4 ± 0.28^{a}	1.99 ± 0.53^{abcd}

		1%	104.6 ± 4.7^{a}	0.96 ± 0.72^{a}	407.72 ± 11.16^{a}	3.67 ± 0.18^{b}	2.13 ± 0.08^{abcd}
	AL-N	2%	100.5 ±5.2^{a}	2.52 ± 1.21^{a}	415.78 ± 13.52^{a}	2.34 ± 0.77^{a}	2.25 ± 0.65^{acd}
		3%	104.4 ± 1.8^{a}	2.34 ± 0.52^{a}	406.67 ± 5.52^{a}	2.24 ± 0.27^{a}	2.55 ± 0.23^{a}
		1%	101.0 ± 1.3^{a}	2.12 ± 1.43^{a}	424.89 ± 8.10^{a}	1.28 ± 0.14^{c}	1.20 ± 0.024^{bcd}
	AL-Z	2%	102.9 ± 1.5^{a}	3.58 ± 0.44^{a}	428.61 ± 2.04^{a}	1.19 ± 0.039^{c}	1.27 ± 0.12^{cd}
		3%	110.3 ± 3.4^{a}	3.68 ± 1.10^{a}	429.22 ± 2.53^{a}	1.15 ± 0.17^{c}	1.46 ± 0.014^{d}
		P-values					
		Starch	0.524	0.071	0.004*	<0.001*	<0.001*
		Concentration	0.181	0.030*	0.704	0.002*	0.300
		Starch : Concentration	0.332	0.620	0.248	<0.001*	0.070
		AL-0%	99.5 ± 6.5^{a}	23.86 ± 6.76^{a}	395.89 ± 5.59^{a}	4.76 ± 0.16^{a}	3.21 ± 0.96^{a}
		1%	99.5 ± 7.7^{a}	24.17 ± 5.24^{a}	398.83 ± 3.75^{a}	4.08 ± 0.62^{abc}	3.27 ± 0.72^{a}
	AL-N	2%	102.8 ± 3.6^{a}	22.12 ± 2.79^{a}	400.89 ± 2.59^{a}	4.48 ± 0.90^{a}	3.65 ± 0.81^{a}
P2		3%	104.3 ± 1.4^{a}	20.34 ± 2.28^{a}	405.22 ± 3.14^{a}	4.12 ± 0.13^{abc}	4.05 ± 0.47^{a}
		1%	83.4 ± 8.4^{abc}	30.52 ± 2.19^{a}	400.78 ± 8.68^{a}	3.82 ± 0.47^{abc}	3.20 ± 0.28^{a}
	AL-Z	2%	57.9 ± 15.8^{bc}	29.38 ± 4.19^{a}	403.78 ± 2.45^{a}	2.87 ± 0.34^{bc}	3.05 ± 0.60^{a}
		3%	68.5 ± 17.9^{c}	30.90 ± 1.88^{a}	402.83 ± 13.10^{a}	2.59 ± 0.93^{c}	3.04 ± 1.2^{a}
		P-values					
		Starch	<0.001*	0.004*	0.823	0.002*	0.220
		Concentration	0.028*	0.615	0.200	0.003*	0.888
		Starch : Concentration	0.006*	0.257	0.902	0.042*	0.677
		AL-0%	80.5 ± 17.6^{ab}	32.28 ± 1.98^{a}	401.11 ± 4.94^{a}	3.13 ± 0.19^{a}	1.52 ± 0.19^{a}
		1%	81.3 ± 11.8^{ab}	36.57 ± 3.18^{a}	406.44 ± 2.38^{a}	2.87 ± 0.96^{a}	1.37 ± 0.24^{a}
	AL-N	2%	77.1 ± 3.7^{ab}	35.67 ± 2.45^{a}	409.61 ± 3.67^{a}	2.48 ± 0.35^{acd}	1.32 ± 0.06^{a}
P3		3%	84.5 ± 5.5^{a}	31.85 ± 0.94^{a}	412.11 ± 2.43^{a}	1.78 ± 0.29^{bcde}	1.12 ± 0.19^{a}
		1%	57.5 ± 16.1^{ab}	34.39 ± 2.48^{a}	412.56 ± 2.59^{a}	1.54 ± 0.29^{cde}	1.51 ± 0.31^{a}
	AL-Z	2%	43.1 ± 24.2^{ab}	29.67 ± 5.64^{a}	412.78 ± 0.09^{a}	1.63 ± 0.37^{de}	1.39 ± 0.19^{a}
		3%	39.4 ± 14.8^{b}	29.30 ± 10.86^{a}	411.99 ± 9.78^{a}	1.20 ± 0.30^{e}	1.17 ± 0.21^{a}
		P-values					
		Starch	<0.001*	0.187	0.249	<0.001*	0.448
		Concentration	0.128	0.378	0.003*	<0.001*	0.034*
		Starch : Concentration	0.108	0.749	0.625	0.102	0.946

**Samples with the same letter do not have a statistically significant difference. Samples with a different letter have significant differences.

*Effects statistically significant (p-value < 0.05)

Moreover, the addition of the AL-Z filler caused a significant change in the con-tact angle of polyurethanes P2 and P3, increasing their hydrophilicity. That phenomenon could be

explained by the inhibition of soft segment crystallization with the inclusion of AL-Z, which enables PEG to migrate to the surface. These results are analogous to the phenomena exposed by Kumar., et al. [56], who attributed the increase in the contact angle to a strong intermolecular hydrogen bonding between the cellulose nanofiber (filler) and the polyurethane matrix, enlarging the crystallinity of soft segments and the migration of hydrophobic groups to the surface of composites. The improvement in the hydrophilicity of the composite material makes it more attractive for cardiovascular applications due to its anti-fouling property. This property is associated with a major hydrophilic surface with the capacity to form a tiny layer of water that prevents the adhesion of platelets and proteins, which induce thrombus formation [57]; therefore, composite materials with AL-Z are candidates for application in the cardiovascular field. AL-N filler in all PU matrices and AL-Z for P1 did not affect the contact angle to a significant degree.

The evaluation of the hydrophilicity of PU composites was complemented with the study of swelling behavior that was examined by water absorption. The weight change of samples related to the time they were soaked in water and the area under the curve are presented in Figure 2-4 and Table 2-2. From Table 2-2, it was observed that polyurethane matrices without filler exhibited statistical differences, in which P2 and P3 showed a large area under the curve than P1. This area un-der the curve is associated with the capacity of polyurethane matrices to uptake water, considering the 80 h time frame. Then, P2 and P3 have a greater capacity to uptake water in comparison with P1. This result is assigned with the concentration of PEG, which enlarges the number of hydrophilic groups (ether groups) in the polyurethane backbone, improving the hydrophilicity of composites [54,58].

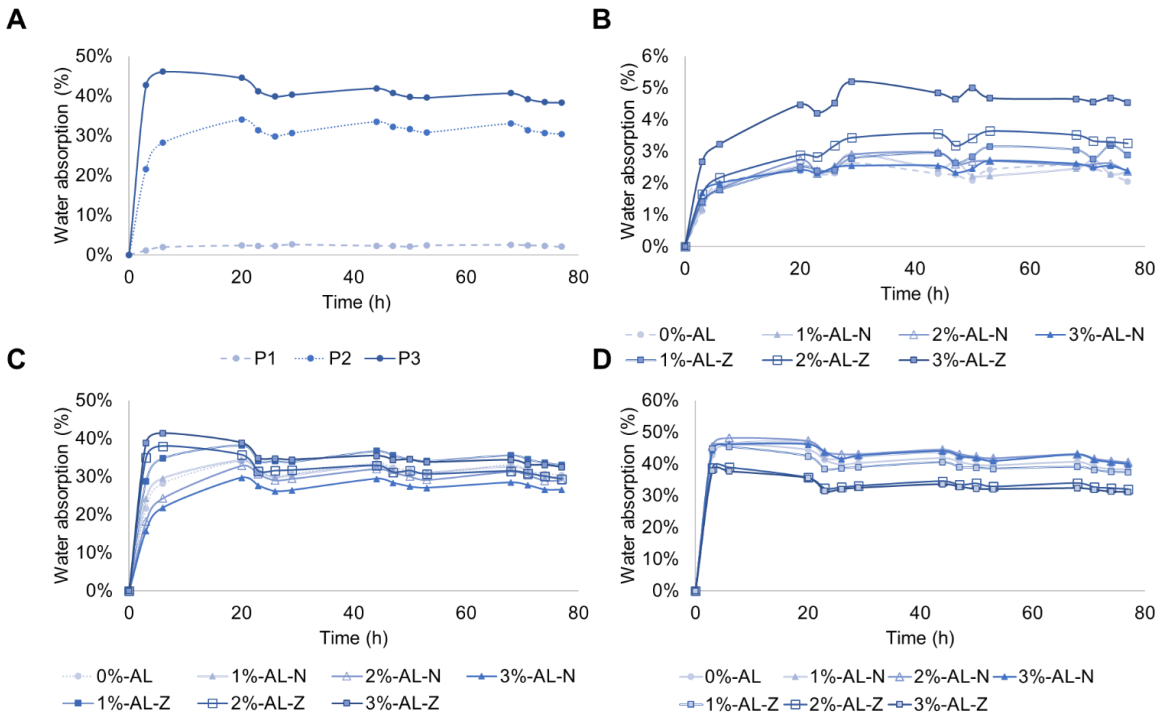

Figure 2-4. *Water absorptions of (A) PU matrices without fillers, (B) P1, (C) P2 and (D) P3 composites*

From Figure 2-4A - Figure 2-4D, composite materials reach the maximum water absorption within the first 30 h. P1 composite polyurethanes were the last materials to achieve the maximum water up-take (29 h) after P2 (20 h) and P3 (6 h). This behavior is associated with the crosslinking density and crystalline structure of segments, which modulate the resistance of the diffusivity of solvents inside the material [34,59]. Therefore, P1 composites take more time to reach a swelling equilibrium due to the semicrystalline PCL structure, followed by the P2 crosslinked structures and P3 materials, which contain the lowest PCL and PE (crosslinking agent) concentration in comparison with P2 and P1. Similar results were obtained by Fonseca., et al. [59], who synthesized crosslinked polyurethanes from PCL and PEG, finding that an increase in crosslinked density and PCL concentration reduces the water uptake. On the other hand, adding fillers in polyurethane matrices did not have a different statistical significance. That phenomena could be due to the concentration of zwitterionic groups in composites were not significant to increase ionic strength that allows the improvement of water absorption.

The thermal stability of composites was evaluated by thermogravimetric analysis (TGA). Figure A **7** shows the weight loss of materials with the increment of temperature. Figure A **7**A-Figure A 7D exhibit one step of degradation for all composite materials, and it occurs in the same interval of temperature (270 – 457 °C). This phenomenon could be explained by the degradation of starches that takes place between 260 – 400 °C [60], followed by the endothermic decomposition of polyurethane that happens between 310 – 380 °C [61]. The degradation of polyurethane occurs principally in three steps. First, urethane bonds and hard segments are broken up, followed by the crosslinker's decomposition and, finally, the degradation of polyols due to the effect of temperature [31]. The temperature at which the maximum rate of degradation (Tmax) occurs (as reported in Table 2-2) did not show a statistically significant difference between polyurethane matrices with and without the inclusion of fillers (AL-N and AL-Z). Thus, the addition of starches in polyurethane matrices does not affect their thermal stability [60,61]. These results are consistent with the investigation carried out by Swamy., et al. [60], who used starch as a filler, with starch loading concentrations of 5 – 25% in polymeric matrices, and concluded that the thermal stability of composites was not affected.

Results from the tensile/strain assay were reported in Table 2-2. Mechanical properties changed when the compositions of polymeric matrices were modified, in fact, P2 has greater tensile strength (4.76 ± 0.16 MPa) and secant module (3.21 ± 0.96 MPa) than P1 (σ=2.4 ± 0.28, E=1.99 ± 0.53) and P3 (σ=3.13 ± 0.19, E=1.52 ± 0.19). This could be explained by the change in hard segments, in which an enlarged concentration of hard domains causes an increase in tensile strength; in contrast, the enlargement of soft segments decreases the stiffness of polymeric material [31]. Similar results were obtained by Alquichire., et al. [31], who made a design mixture of PEG, PCL, and PE and described a similar effect with the change in polyol composition and crosslinker.

The addition of starches (AL-N and AL-Z) influenced the mechanical properties. Tensile strength decreased in a significant degree when AL-Z was added to polymer matrices; additionally, the inclusion of AL-N did not present a different statistical significance in tensile strength (except for P1-1% AL-N which increased), as can be noted in Table 2-2. This

behavior is attributed to the thermodynamic compatibility between fillers and polyurethane matrices, which allude to the capacity to form hydrogen bonding at the interface, that intermolecular interactions adhere the surface of filler to the polymeric matrix, permitting the energy transmission on the boundaries of each material, then AL-Z acts as an inert material caused to not formations of hydrogen bonding at the interface with polyurethane in comparison with AL-N; therefore, starch modified with a zwitterion moiety creates defected areas that do not allow the transmission of energy when the composite is stretched, decreasing the tensile strength [51,62,63]. Furthermore, the reduction in tensile strength of P1 composites filled with a concentration of AL-N that is greater than 1% wt indicates that the increase in the filler inside the polyurethane matrix permits formations of agglomerates and voids inside these agglomerates (Figure 2-5), which reduce specific contact area at the interface filler-matrix [64]. These results are consistent with similar behavior reported in the literature for composite materials [51,62–64].

The reported tensile strength and strain at failure (%) of the femoral artery are 1 MPa and 76%, respectively. The composites synthetized in this work could be applied for the fabrication of synthetic vascular grafts since all the materials have a tensile strength and strain at failure above 1MPa and 76%, respectively [65].

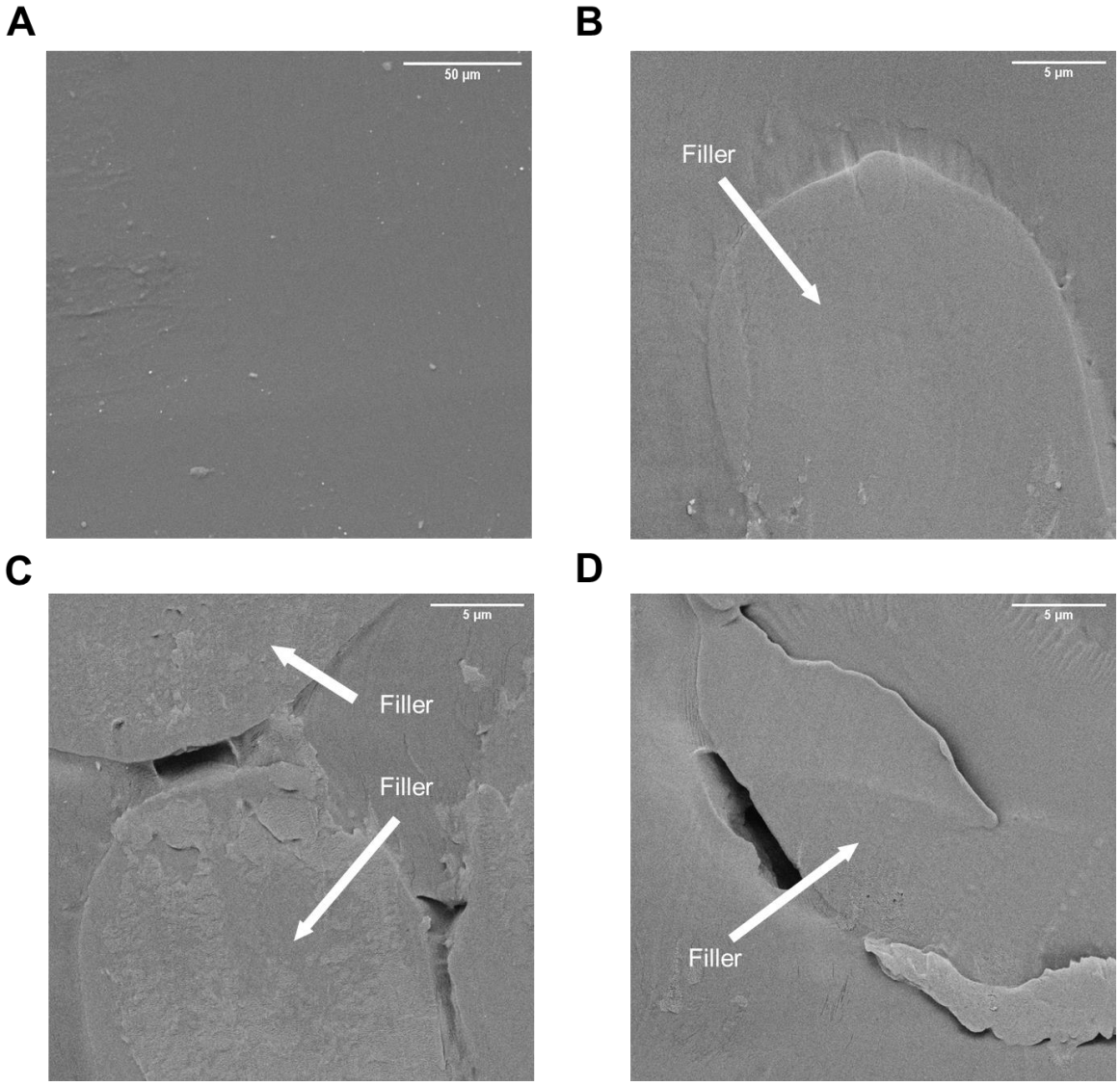

***Figure 2-5**. Representatives SEM images of P1 polyurethane composites at (A) 0%-AL, (B) 1%-AL-N, (C) 2%-AL-N, and (D) 3%-AL-N*

The dynamic mechanical analysis recorded the loss factor (tan δ), storage modulus (E'), and loss modulus (E"). With the loss factor of matrices (Figure 2-6) and composites polyurethanes (Figure A 8)), the segregation of the hard and soft domains of materials was established. From Figure 2-6, it was noted that P1 had a homogeneous phase distribution due to the presence of one peak in tan δ. This result is due to the polarity of polycaprolactone diol (PCL), which permits ester groups to interact with urethane groups, making the generation of hydrogen bonding possible. This is consistent with the results reported by Asensio., et al.

[66], who studied the effect of different polyols (carbonates, esters, and ethers) on the separation of microphases (hard and soft segments) and their relationship with mechanical properties.

On the other hand, polyurethane matrices P2 and P3 showed a previous formation of a plateau form in the curve before the maximum value of tan δ. This result is caused by a partial mixture of soft and hard domains, principally due to the increase in cross-linking, which decreases the mobility of chains in the polyurethane backbone, and this phenomenon is attributed to an enlarged concentration of PE in the formulation of polymeric matrices. Furthermore, comparing polyurethane matrices P1 and P3, the increment in the concentration of PEG generated the segregation of soft and hard segments, produced by a lower polarity of PEG than PCL; additionally, this behavior is complemented by the reduction in the hydrogen bonding number that could be formed between a polar polyol such as PCL with urethane groups [31,66,67]. From Figure A 8, it can be seen that adding filler in polymeric matrices did not affect the distribution of soft and hard segments compared with matrices lacking fillers.

The maximum storage modulus in the glassy region (Max E') reported in Table 2-3 shows that the inclusion of AL-Z in polyurethane matrices P2 and P3 has the largest statistically significant value compared with polyurethane matrices with AL-N and without fillers. This could be explained by the theory of dual nanolayers formed around fillers, where a primary layer conformed by crosslinker chains is formed near particles, followed by a second layer that is assigned to chains that are less bounded [68]. Then, an enlarged storage modulus could be associated with an increase in interactions between chains that are crosslinkers in the first layer. Additionally, the glass transition temperature (Tg) is reported as the temperature which occurs at the maximum change of the storage modulus and is shown in Table 2-3. From these data, statically less Tg was noted for polyurethane composites P2 and P3 with AL-Z compared with P2 and P3 with AL-N and without fillers. This phenomenon is attributed to a reduction in the crystallinity region, which is related to improving chains mobility in bulk polymers. These results are consistent with those reported in the literature [21,69].

Differential Scanning Calorimetry (DSC) was used to study the thermal transitions of composites. Thermograms of polyurethanes are showed in Figure 2-6B and Figure A 9 where materials exhibit only a glass transition. These glass transition temperatures (Table 2-3) were between -50.2 °C to -40.3 °C. Therefore, Tg from DMA and DSC indicate that composite materials are in the rubbery region at ambient temperature (12 °C – 20 °C) [70].

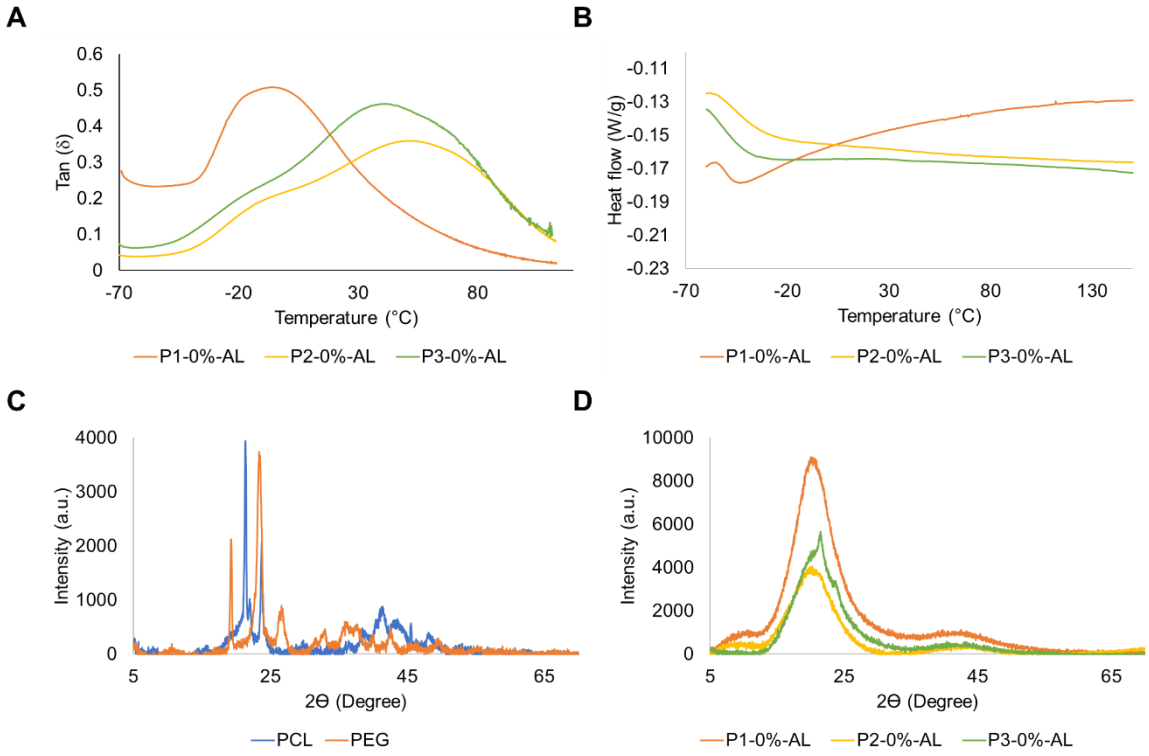

Figure 2-6. *(A) Loss factor, (B) DSC of polyurethane matrices without fillers and XRD spectra of (C) polyols and (D) polymeric matrices*

XRD spectra of polyols and polyurethane matrices without and with fillers are shown in Figure 2-6C, Figure 2-6D, and Figure A 10. From Figure 2-6C, it can be seen that PEG (peaks at 2Θ=19.3°, 23.5°, and 26.8°) and PCL (peaks at 2Θ=21.3° and 23.7°) are semicrystalline polyols; additionally, amorphous polyurethane matrices exhibited a peak between 19°< 2Θ < 22° that can be assigned to crystalline regions conferred by PCL and PEG segments (Figure 2-6D). Variations in the concentrations of polyols change the intensity in the peak for polyurethane matrices, where P1 has the largest intensity due to a major concentration of PCL compared with P2 and P3. Furthermore, the inclusion of PE in polyurethane matrices

caused a reduction in the intensity of this peak, and this could be attributed to a suppression of PCL and PEG crystalline segments. Additionally, the increase of PE (crosslinker) concentration did not allow the formation of a linear segmented polymer, which can show an order in their structure in contrast with crosslinking molecular structures. These results are similar to XRD spectra reported in the literature for polyurethanes obtained by PCL and PEG [31,71].

***Table 2-3**. Maximum storage modulus (Max E'), glass transition temperature (Tg) obtained from DMA and DSC, and degree of crystallinity (DC) of composite polyurethanes.*

PU	Starch	Concentration	Max E' (MPa)**	Tg from DMA (°C)**	Tg from DSC (°C)	DC (%)
P1	AL-N	AL-0%	3004 ± 1508^{a}	-32.89 ± 0.74^{a}	-46.7	73.6%
		1%	3042 ± 697^{a}	-32.65 ± 0.39^{a}	-47.7	63.7%
		2%	2703 ± 1357^{a}	-33.02 ± 0.42^{a}	-46.8	63.2%
		3%	3041 ± 729^{a}	-33.61 ± 0.80^{a}	-47.7	68.9%
	AL-Z	1%	3297 ± 127^{a}	-33.75 ± 1.75^{a}	-50.2	68.9%
		2%	3328 ± 388^{a}	-34.83 ± 0.82^{a}	-49.7	54.1%
		3%	3512 ± 647^{a}	-35.80 ± 2.05^{a}	-49.2	72.3%
	P-values					
	Starch		0.334	0.045*	-	-
	Concentration		0.890	0.052	-	-
	Starch : Concentration		0.922	0.682	-	-
P2	AL-N	AL-0%	4054 ± 274^{a}	-24.94 ± 1.77^{a}	-42.7	64.2%
		1%	4708 ± 702^{a}	-28.90 ± 1.41^{a}	-41.9	69.2%
		2%	4513 ± 617^{a}	-24.28 ± 1.42^{a}	-40.3	59.3%
		3%	4668 ± 455^{a}	-24.28 ± 1.26^{a}	-39.8	61.8%
	AL-Z	1%	9588 ± 2903^{bcd}	-38.69 ± 4.43^{bcd}	-48.4	71.1%
		2%	8537 ± 3620^{cd}	-40.23 ± 2.83^{cd}	-44.2	72.4%
		3%	6447 ± 451^{d}	-41.36 ± 5.86^{d}	-40.3	66.8%
	P-values					
	Starch		<0.001*	<0.001*	-	-
	Concentration		0.012*	0.012*	-	-
	Starch : Concentration		0.013*	0.014*	-	-
P3	AL-N	AL-0%	4913 ± 328^{a}	-35.16 ± 0.92^{a}	-48.0	71.3%
		1%	6791 ± 2084^{ab}	-41.01 ± 1.61^{ab}	-48.1	60.6%

	2%	5744 ± 40^{ab}	-41.48 ± 1.65^{ab}	-48.1	69.0%
	3%	6045 ± 1936^{ab}	-38.00 ± 1.75^{a}	-48.2	70.5%
	1%	7981 ± 2676^{ab}	-40.66 ± 1.88^{ab}	-47.8	69.4%
AL-Z	2%	8401 ± 1882^{ab}	-40.86 ± 5.03^{ab}	-48.3	72.1%
	3%	11694 ± 3883^{b}	-45.36 ± 0.46^{b}	-48.2	66.7%
P-values					
Starch		0.021*	0,092	-	-
Concentration		0.037*	<0.001*	-	-
Starch : Concentration		0.215	0.043*	-	-

The crystallinity degree (DC) of composite polyurethanes shown in Table 2-3 confirmed that the inclusion of AL-N and AL-Z in polyurethane matrices reduced the crystalline regions due to the disruption of interactions inside soft segments. Marand., et al. [72] obtained analogous results with the inclusion of hydroxyapatite nanoparticles in polyurethane matrices with PCL-diol.

2.4. Conclusions

Composite PUs were synthesized and confirmed by FTIR. Also, these materials were characterized in terms of their physicochemical, mechanical, and thermal properties, where the interaction of polyurethane matrices with fillers depends on the concentrations of soft and hard segments. FTIR showed that AL-N interacts with soft domains and AL-Z with hard segments. From contact angle and swelling assay, AL-Z increases the hydrophilicity nature of polyurethane matrices P2 and P3. Tensile/strain assay shows that AL-N improves tensile strength until 1% wt; on the contrary, AL-Z reduces that value for all PUs matrices. SEM images confirm agglomerations of fillers and voids between these agglomerates. TGA exhibited that fillers did not affect the thermal stability. Finally, DSC, DMA, and XRD showed that fillers reduce the crystallinity of PUs matrices due to the formation of defects at filler-matrix interface and the disruption of short-range intermolecular interactions, reflected in the reduction of Tg and DC.

2.5. References

1. Toh HW, Toong DWY, Ng JCK, Ow V, Lu S, Tan LP, et al. Polymer blends and polymer composites for cardiovascular implants. Eur Polym J. 2021, 146.

2. Haponiuk JT, Formela K. PU Polymers, Their Composites, and Nanocomposites: State of the Art and New Challenges [Internet]. Polyurethane Polymers: Composites and Nanocomposites. Elsevier Inc.; 2017. 1–20 p.

3. Zieber L, Or S, Ruvinov E, Cohen S. Microfabrication of channel arrays promotes vessel-like network formation in cardiac cell construct and vascularization in vivo. Biofabrication [Internet]. 2014;6(2), 24102.

4. Díaz-Herráez P, Garbayo E, Simón-Yarza T, Formiga FR, Prosper F, Blanco-Prieto MJ. Adipose-derived stem cells combined with Neuregulin-1 delivery systems for heart tissue engineering. Eur J Pharm Biopharm [Internet]. 2013;85(1), 143–150.

5. Yu C, Yang H, Wang L, Thomson JA, Turng LS, Guan G. Surface modification of polytetrafluoroethylene (PTFE) with a heparin-immobilized extracellular matrix (ECM) coating for small-diameter vascular grafts applications. Mater Sci Eng C [Internet]. 2021;128(June), 112301.

6. Mora-Cortes LF, Rivas-Muñoz AN, Neira-Velázquez MG, Contreras-Esquivel JC, Roger P, Mora-Cura YN, et al. Biocompatible enhancement of poly(ethylene terephthalate) (PET) waste films by cold plasma aminolysis. J Chem Technol Biotechnol [Internet]. 2022.

7. Kianpour G, Bagheri R, Pourjavadi A, Ghanbari H. In situ synthesized TiO2-polyurethane nanocomposite for bypass graft application: In vitro endothelialization and degradation. Mater Sci Eng C [Internet]. 2020;114(May), 111043.

8. Lee TH, Yen CT, Hsu SH. Preparation of Polyurethane-Graphene Nanocomposite and Evaluation of Neurovascular Regeneration. ACS Biomater Sci Eng. 2020;6(1), 597–609.

9. Obiweluozor FO, Emechebe GA, Kim DW, Cho HJ, Park CH, Kim CS, et al. Considerations in the Development of Small-Diameter Vascular Graft as an Alternative for Bypass and Reconstructive Surgeries: A Review. Cardiovasc Eng Technol. 2020;11(5), 495–521.

10. Gostev AA, Karpenko AA, Laktionov PP. Polyurethanes in cardiovascular prosthetics. Polym Bull [Internet]. 2018;75(9), 4311–4325.

11. Navas-Gómez K, Valero MF. Why polyurethanes have been used in the manufacture and design of cardiovascular devices: A systematic review. Materials (Basel). 2020;13(15), 1–17.

12. Arévalo-Alquichire S, Morales-Gonzalez M, Diaz LE, Valero MF. Surface response methodology-based mixture design to study the influence of polyol blend composition on polyurethanes' properties. Molecules. 2018;23(8).

13. Adipurnama I, Yang M-C, Ciach T, Butruk-Raszeja B. Surface modification and endothelialization of polyurethane for vascular tissue engineering applications: A review. Biomater Sci. 2017;5(1), 22–37.

14. Król P, Uram Ł, Król B, Pielichowska K, Sochacka-Piętal M, Walczak M. Synthesis and property of polyurethane elastomer for biomedical applications based on nonaromatic isocyanates, polyesters, and ethylene glycol. Colloid Polym Sci. 2020;298(8), 1077–1093.

15. Li G, Li D, Niu Y, He T, Chen KC, Xu K. Alternating block polyurethanes based on PCL and PEG as potential nerve regeneration materials. J Biomed Mater Res - Part A. 2014;102(3), 685–697.

16. Vadillo J, Larraza I, Calvo-Correas T, Gabilondo N, Derail C, Eceiza A. Role of in situ added cellulose nanocrystals as rheological modulator of novel waterborne polyurethane urea for 3D-printing technology. Cellulose [Internet]. 2021;28(8), 4729–4744.

17. Bharadwaz A, Jayasuriya AC. Recent trends in the application of widely used natural and synthetic polymer nanocomposites in bone tissue regeneration. Mater Sci Eng C [Internet]. 2020;110(January), 110698.

18. Villani M, Consonni R, Canetti M, Bertoglio F, Iervese S, Bruni G, et al. Polyurethane-based composites: Effects of antibacterial fillers on the physical-mechanical behavior of thermoplastic polyurethanes. Polymers (Basel). 2020;12(2).

19. Arévalo FR, Osorio SA, Valcárcel NA, Ibarra JC, Valero MF. Characterization and in vitro biocompatibility of binary mixtures of chitosan and polyurethanes synthesized from chemically modified castor oil, as materials for medical use. Polym from Renew Resour. 2018;9(1), 23–38.

20. Hormaiztegui MEV, Marin D, Gañán P, Stefani PM, Mucci V, Aranguren MI. Nanocelluloses reinforced bio-waterborne polyurethane. Polymers (Basel). 2021;13(17).

21. Gaaz TS, Sulong AB, Ansari MNM, Kadhum AAH, Al-Amiery AA, Nassir MH. Effect of starch loading on the thermo-mechanical and morphological properties of polyurethane composites. Materials (Basel). 2017;10(7).

22. Torres FG, Commeaux S, Troncoso OP. Starch-based biomaterials for wound-dressing applications. Starch/Staerke. 2013;65(7–8), 543–551.

23. Carvalho AJF. Starch: Major sources, properties and applications as thermoplastic materials. Monomers, Polym Compos from Renew Resour. 2008, 321–342.

24. Jin M, Shi J, Zhu W, Yao H, Wang DA. Polysaccharide-Based Biomaterials in Tissue Engineering: A Review. Tissue Eng - Part B Rev. 2021;27(6), 604–626.

25. Zia F, Zia KM, Zuber M, Kamal S, Aslam N. Starch based polyurethanes: A critical review updating recent literature. Carbohydr Polym [Internet]. 2015;134, 784–798.

26. Zheng L, Sun Z, Li C, Wei Z, Jain P, Wu K. Progress in biodegradable zwitterionic materials. Polym Degrad Stab [Internet]. 2017;139, 1–19.

27. Wang J, Sun H, Li J, Dong D, Zhang Y, Yao F. Ionic starch-based hydrogels for the prevention of nonspecific protein adsorption. Carbohydr Polym. 2015;117, 384–391.

28. Wang J, Li J, Yang H, Zhu C, Yang J, Yao F. Preparation and characterization of protein resistant zwitterionic starches: The effect of substitution degrees. Starch/Staerke. 2015;67(11–12), 920–929.

29. Liu Y, Yang L, Ma C, Zhang Y. Thermal behavior of sweet potato starch by non-isothermal thermogravimetric analysis. Materials (Basel). 2019;12(5).

30. Arévalo F, Uscategui YL, Diaz L, Cobo M, Valero MF. Effect of the incorporation of chitosan on the physico-chemical, mechanical properties and biological activity on a mixture of polycaprolactone and polyurethanes obtained from castor oil. J Biomater Appl. 2016;31(5), 708–720.

31. Arévalo-Alquichire S, Morales-Gonzalez M, Navas-Gómez K, Diaz LE, Gómez-Tejedor JA, Serrano MA, et al. Influence of polyol/crosslinker blend composition on phase separation and thermo-mechanical properties of polyurethane thin films. Polymers (Basel). 2020;12(3).

32. Morales-Gonzalez M, Arévalo-Alquichire S, Diaz LE, Sans JÁ, Vilarinõ-Feltrer G, Gómez-Tejedor JA, et al. Hydrolytic stability and biocompatibility on smooth muscle cells of polyethylene glycol-polycaprolactone-based polyurethanes. J Mater Res [Internet]. 2020;35(23–24):3276–3285.

33. Valero MF, Díaz LE. Polyurethane networks from pentaerythritol-modified castor oil and lysine polyisocyanates: synthesis, mechanical, and thermal properties and in vitro degradation. Quim Nova [Internet]. 2014; 37(9):1441–1445.

34. Uscátegui YL, Arévalo-Alquichire SJ, Gómez-Tejedor JA, Vallés-Lluch A, Díaz LE, Valero MF. Polyurethane-based bioadhesive synthesized from polyols derived from castor oil (Ricinus communis) and low concentration of chitosan. J Mater Res. 2017;32(19), 3699–3711.

35. Jin Y, Zhu Z, Liang L, Lan K, Zheng Q, Wang Y, et al. A facile heparin/carboxymethyl chitosan coating mediated by polydopamine on implants for hemocompatibility and antibacterial properties. Appl Surf Sci. 2020;528, 146539.

36. Zhao H, Li KC, Wu W, Li Q, Jiang Y, Cheng BX, et al. Microstructure and viscoelastic behavior of waterborne polyurethane/cellulose nanofiber nanocomposite. J Ind Eng Chem [Internet]. 2022;110:150–157.

37. Chi H, Xu K, Wu X, Chen Q, Xue D, Song C, et al. Effect of acetylation on the properties of corn starch. Food Chem. 2008;106(3), 923–928.

38. Pigłowska M, Kurc B, Rymaniak Ł, Lijewski P, Fuć P. Kinetics and thermodynamics of thermal degradation of different starches and estimation the OH group and H2O content on the surface by TG/DTG-DTA. Polymers (Basel). 2020;12(2).

39. Cardoso J, Rubio L, Albores-Velasco M. Thermal degradation of poly(sulfobetaines). J Appl Polym Sci. 1999;73(8), 1409–1414.

40. Li M, Chen J, Li L, Ye C, Lin X, Qiu T. Novel multi–SO3H functionalized ionic liquids as highly efficient catalyst for synthesis of biodiesel. Green Energy Environ [Internet]. 2021;6(2), 271–282.

41. Dereszewska A, Olayo R, Cardoso J. Synthesis and Thermal Degradation of Poly(n-butylisocyanate) Modified by 1,3-Propanesultone. J Appl Polym Sci. 2003;90(13), 3594–3601.

42. Liu J, Zhong L, Zewen Y, Liu Y, Meng X, Zhang W, et al. High-efficiency emulsification anionic surfactant for enhancing heavy oil recovery. Colloids Surfaces A Physicochem Eng Asp [Internet]. 2022;642, 128654.

43. Yan Y, Peng B, Niu B, Ji X, He Y, Shi M. Understanding the Structure, Thermal, Pasting, and Rheological Properties of Potato and Pea Starches Affected by Annealing Using Plasma-Activated Water. Front Nutr. 2022;9, 1–13.

44. Fonseca-Santanilla EB, Betancourt-López LL. Physicochemical and structural characterization of starches from Andean roots and tubers grown in Colombia. Food Sci Technol Int. 2022;28(2), 144–156.

45. Govindaraju I, Sunder M, Chakraborty I, Mumbrekar KD, Sankar Mal S, Mazumder N. Investigation of physico-chemical properties of native and gamma irradiated starches. Mater Today Proc [Internet]. 2022;55, 12–16.

46. Ferraz CA, Fontes RLS, Fontes-Sant'Ana GC, Calado V, López EO, Rocha-Leão MHM. Extraction, Modification, and Chemical, Thermal and Morphological Characterization of Starch From the Agro-Industrial Residue of Mango (Mangifera indica L) var. Ubá. Starch/Staerke. 2019;71(1–2).

47. Wongsamut C, Suwanpreedee R, Manuspiya H. Thermoplastic polyurethane-based polycarbonate diol hot melt adhesives: The effect of hard-soft segment ratio on adhesion properties. Int J Adhes Adhes [Internet]. 2020;102, 102677.

48. Kasprzyk P, Benes H, Donato RK, Datta J. The role of hydrogen bonding on tuning hard-soft segments in bio-based thermoplastic poly(ether-urethane)s. J Clean Prod [Internet]. 2020;274, 122678.

49. Zhao X, Qi Y, Li K, Zhang Z. Hydrogen bonds and FTIR peaks of polyether polyurethane-urea. Key Eng Mater. 2019;815 KEM, 151–156.

50. Shameli K, Ahmad M Bin, Jazayeri SD, Sedaghat S, Shabanzadeh P, Jahangirian H, et al. Synthesis and characterization of polyethylene glycol mediated silver nanoparticles by the green method. Int J Mol Sci. 2012;13(6), 6639–6650.

51. Malay O, Oguz O, Kosak C, Yilgor E, Yilgor I, Menceloglu YZ. Polyurethaneurea-silica nanocomposites: Preparation and investigation of the structure-property behavior. Polymer (Guildf) [Internet]. 2013;54(20), 5310–5320.

52. Lee HS, Hsu SL. An analysis of phase separation kinetics of model polyurethanes. Macromolecules [Internet]. 1989 Mar 1;22(3), 1100–1105.

53. Vakili H, Mohseni M, Makki H, Yahyaei H, Ghanbari H, González A, et al. Synthesis of segmented polyurethanes containing different oligo segments: Experimental and computational approach. Prog Org Coatings. 2021;150.

54. Li L, Liu X, Niu Y, Ye J, Huang S, Liu C, et al. Synthesis and wound healing of alternating block polyurethanes based on poly(lactic acid) (PLA) and poly(ethylene glycol) (PEG). J Biomed Mater Res - Part B Appl Biomater. 2017;105(5):1200–1209.

55. Walter PA, Gnanasekaran D, Reddy BSR. Synthesis of different soft segmented polyurethane membranes: Structural characterization and antimicrobial activity studies. J Polym Mater. 2014;31(3), 305–316.

56. Kumar S, Tewatia P, Samota S, Rattan G, Kaushik A. Ameliorating properties of castor oil based polyurethane hybrid nanocomposites via synergistic addition of graphene and cellulose nanofibers. J Ind Eng Chem [Internet]. 2022;109, 492–509.

57. Erathodiyil N, Chan H-M, Wu H, Ying JY. Zwitterionic polymers and hydrogels for antibiofouling applications in implantable devices. Mater Today [Internet]. 2020;38, 84–98.

58. Yang Z, Wu G. Effects of soft segment characteristics on the properties of biodegradable amphiphilic waterborne polyurethane prepared by a green process. J Mater Sci [Internet]. 2020;55(7), 3139–3156.

59. Polo Fonseca L, Bergamo Trinca R, Isabel Felisberti M. Thermo-responsive polyurethane hydrogels based on poly(ethylene glycol) and poly(caprolactone): Physico-chemical and mechanical properties. J Appl Polym Sci. 2016;133(25), 1–10.

60. Kendaganna Swamy BK, Siddaramaiah. Structure-property relationship of starch-filled chain-extended polyurethanes. J Appl Polym Sci [Internet]. 2003;90(11, :2945–2954.

61. Omidi-Ghallemohamadi M, Jafari P, Behniafar H. Polyurethane elastomer–silica hybrid films based on oxytetramethylene soft segments: thermal and thermo-mechanical investigations. J Polym Res [Internet]. 2021; 28(3), 3.

62. Weng F, Zhang P, Koranteng E, Zhang Y, Wu Q, Zeng G. Effects of shell powder size and content on the properties of polycaprolactone composites. J Appl Polym Sci. 2021;138(43), 1–11.

63. Vrsaljko D, Blagojević SL, Leskovac M, Kovačević V. Effect of calcium carbonate particle size and surface pretreatment on polyurethane composite Part I: Interface and mechanical properties. Mater Res Innov. 2008;12(1), 40–46.

64. Bharadwaj-Somaskandan S, Krishnamurthi B, Sergeeva T, Shutov F. Macro- and Microfillers as Reinforcing Agents for Polyurethane Elastomers. J Elastomers Plast. 2003;35(4), 325–334.

65. Hasan A, Memic A, Annabi N, Hossain M, Paul A, Dokmeci MR, et al. Electrospun scaffolds for tissue engineering of vascular grafts. Acta Biomater [Internet]. 2014;10(1), 11–25.

66. Asensio M, Costa V, Nohales A, Bianchi O, Gómez CM. Tunable structure and properties of segmented thermoplastic polyurethanes as a function offlexible segment. Polymers (Basel). 2019;11(12), 1–22.

67. Cui Y, Wang H, Pan H, Yan T, Zong C. The effect of mixed soft segment on the microstructure of thermoplastic polyurethane. J Appl Polym Sci. 2021;138(45), 1–10.

68. Bashir MA. Use of Dynamic Mechanical Analysis (DMA) for Characterizing Interfacial Interactions in Filled Polymers. Solids. 2021;2(1), 108–120.

69. Amirkiai A, Panahi-Sarmad M, Sadeghi GMM, Arjmand M, Abrisham M, Dehghan P, et al. Microstructural design for enhanced mechanical and shape memory performance of polyurethane nanocomposites: Role of hybrid nanofillers of montmorillonite and halloysite nanotube. Appl Clay Sci [Internet]. 2020;198, 105816.

70. Jayanarayanan K, Rasana N, Mishra RK. Dynamic Mechanical Thermal Analysis of Polymer Nanocomposites [Internet]. Vol. 3, Thermal and Rheological Measurement Techniques for Nanomaterials Characterization. Elsevier Inc.; 2017. 123–157 p.

71. Loh XJ, Colin Sng KB, Li J. Synthesis and water-swelling of thermo-responsive poly(ester urethane)s containing poly(ε-caprolactone), poly(ethylene glycol) and poly(propylene glycol). Biomaterials. 2008;29(22), 3185–3194.

72. Jalili Marand M, Rezaei M, Babaie A, Lotfi R. Synthesis, characterization, crystallinity, mechanical properties, and shape memory behavior of polyurethane/hydroxyapatite nanocomposites. J Intell Mater Syst Struct. 2020;31(14), 1662–1675

3. Chapter 3: Assessment of the anti-thrombogenic activity of polyurethane starch composites

This chapter is established the evaluation of the anti-thrombogenicity activity of composites polyurethanes. This property was characterized by the clot formation time, platelet adhesion, protein absorption, TAT complex eliciting, and hemolysis. Additionally, it was evaluated the biocompatibility, related with the capacity to maintain the viability of endothelial (HUVECs) and smooth muscle cells (AoSMC). Polyurethane matrices (P1, P2, and P3) without fillers did not show a statistically significant difference between them (except for protein absorption and blood clotting time). Composites polyurethanes (especially with AL-Z) presented an improvement of the anti-thrombogenic property. On the other hand, these composites (with AL-Z) reduced the viability of endothelial cells and did not affect AoSCM in a significant matter (except for P1, which increased). These results showed that addition of fillers improved certain characteristics of polyurethane matrices and that fact allow to postulated these materials as candidates for cardiovascular applications.

3.1. Introduction

Artificial-Small-Diameter-Blood-Vessels (SDBVs) have been used as a solution for the scarcity of autologous grafts implemented in the Coronary Artery Bypass Graft (CABPG)[1,2]. However, the SDBVs have not yet mimicked the properties of autologous vessels (considered the gold standard for CABPG), especially in their resistance to thrombus formation and biocompatibility in the short and long-term service [3]. This lack of blood compatibility of SDBVs has been reflected in complications during their implantation and function inside the patients, such as thromboembolism, aneurysm, and cardiac tamponade [4].

It has been noted that biomaterials used for cardiovascular applications, especially for cardiovascular grafts, confront the hemostasis system, which refers to the mechanism that conduces the clot formation [5]. Therefore, when these devices disrupt this system, a blood clot is formed, causing the occlusion of the graft and, consequently, the post-CABPG complications [6]. One of the stages of the hemostasis mechanism that is related to biomaterials in cardiovascular applications is the activation of the coagulation cascade. It has been proposed that blood contact materials activate clot formation by protein absorption and their attachment on the surface; also, it regulates the activation of the complement and immunology system, which exacerbate the coagulation cascade and inflammation response [7,8]. The coagulation cascade is principally activated by the interaction with the biomaterial surface, significantly with the absorption and autoactivation of coagulation factor XII and raised by adhesion and activation of platelets [9]. Furthermore, the complement and immunology system activation have been assigned to inflammation response by the activation of neutrophils and macrophages that, in the presence of non-degradable implants, produces granulomas to phagocyte the biomaterial, conducing to chronic inflammation [10]. Therefore, investigations efforts have been focused to find materials that reduce the non-specific protein adsorption, platelet adhesion, and coagulation factors activation [11].

One of the most used polymers in cardiovascular applications has been polyurethanes. This polymer is knowledge for its biocompatibility, good mechanical properties, and easy processing in manufacturing technologies applied for cardiovascular devices [12]. However,

the lack of anti-thrombogenic activity of polyurethanes has caused studies have focused their efforts on improving the antithrombotic property and maintaining this property for long-term service, carrying out chemical backbone modifications [13-15], surface modifications [16-18], and inclusion of fillers in the polymeric matrix [19,20]. Between these modifications, zwitterionic moieties have been a tendency in investigations due to their antifouling properties, which prevent nonspecific adsorption of proteins. Recently, the functionalization of polysaccharides with zwitterion has attracted attention in the field of biomaterials owing to the combination of biodegradability and natural resources of polysaccharides with the antifouling property from zwitterionic moieties [21]. Wang., et al [22] inserted the zwitterion moiety in starch by a Williamson etherification and evaluated their resistance to protein absorption, finding that the functionalization of starch with the zwitterion increased by a significant degree the antifouling property when compared with poly(sulfobetaine methacrylate) (PSBMA).

Our reviewing the trajectory of investigations, to the best of our knowledge, there have not been conducted studies about the inclusion of zwitterionic starch as a filler in polyurethane matrices focused on cardiovascular applications. Therefore, this work evaluated the antithrombogenicity activity (according to ISO 10993-4) of polyurethane composites obtained from polycaprolactone diol (PCL), polyethylene glycol (PEG), pentaerythritol (PE), and isophorone diisocyanate (IPDI), adding potato starch (AL-N) and zwitterionic starch (AL-Z) as a filler. The results indicated that the addition of fillers, especially AL-Z reduces the clot formation related to the concentration of thrombin; also, these composite materials can be candidates to cardiovascular applications. Futher studies are required such as in vivo assays to determine complex interactions of these biomaterials, especially with HUVECs and AoSMC which are key cells in the conservation of antithrombogenic activity due to their mechanism to maintain the hemostasis. .

3.2. Materials and methodology

3.2.1. Materials

Polyurethane composites were used as samples and synthesized according to the methodologic exposed in chapter 2. Micro BCA™ Protein Assay Kit and Triton® X-100 were obtained from Thermo Scientific (Waltham, Massachusetss, USA). CytoTox 96® Non-Radioactive Cytotoxicity Assay kit was provided by Promega (Woods Hollow Road, Madison, USA) and Human Thrombin-Antithrombin Complex ELISA Kit (TAT) by abcam (Cambridge, UK). Sodium Dodecyl Sulfate (SDS), ethanol absolute, calcium chloride anhydrous ($CaCl_2$), and bovine albumin serum (BSA) were purchased from Sigma-Aldrich (St. Louis, MO, USA). 0.9% sodium chloride solution was acquired from Baxter (Deerfield, Illinois, USA). Phosphate Buffer Solution 1X (PBS) was obtained from VWR® (Radnor, PA, USA). Human Umbilical Vein Endothelial Cells (HUVECs), Human Aortic Smooth Muscle Cells (AoSMC), EGM BulletKit and SmGM-2 BulleKit were purchased from Lonza (Basel, Switzerland).

3.2.2. Methodology

3.2.2.1. Collection of human whole blood

Human fresh whole blood was collected from healthy people in venous blood collection tubes with 3.2% buffered sodium citrate to make anticoagulated blood. Also, blood samples were obtained while maintaining aseptic conditions and guaranteed data confidentiality, according to the guidelines established by resolution No. 008430 de 1993 of the Ministry of Health of Colombia and the ethical committee of the Universidad de La Sabana.

3.2.2.2. Whole blood clotting time

The time formation of the clot was evaluated according to the methodology proposed by Punnakitikashem., et al. [23]. Briefly, samples of 6 mm in diameter were sterilized with UV radiation for 1 h and stabilized in PBS for 24 h. Also, recalcified blood (0.0091 M $CaCl_2$) was obtained by mixing anticoagulated blood with 0.1 M $CaCl_2$ solution. Each stabilized sample in 2 mL microcentrifuge tubes was exposed to 50 µL of recalcified blood and incubated at ambient temperature (18 °C – 20 °C) for 10, 20, and 40 min. When exposure

time finished, was added 1.5 mL of distilled water per sample and waited for 5 min. Finally, an aliquot of 200 µL per sample was taken and deposited in a 96-well plate to measure absorbance at 570 nm.

3.2.2.3. Hemolysis

The rupture of red cells was measured according to Xu., et al. [14]. First, samples of composite materials (6 mm in diameter) were sterilized by UV radiation for 1 h and stabilized in PBS for 24 h. Furthermore, stabilized blood solution was made by adding 1.75 mL of anticoagulated blood to 33.25 mL of sterile 0.9% sodium chloride solution. Second, stabilized samples located in 1.5 mL microcentrifuge tubes were exposed to stabilized blood (500 µL/sample) for 2 h at 37 °C and, when exposure time finished, were centrifuged at 1000 g for 10 min. Finally, 100 µL supernatant/sample was taken and measured its absorbance (ABSs) at 570 nm in a microplate reader. Positive control (ABSp) was made by adding 200 µL of anticoagulated blood to 10 mL of distilled water, and negative control (ABSn) by blending 200 µL of anticoagulated blood with 10 mL of a sterile 0.9% sodium chloride solution. The percentage of hemolysis was calculated by equation 1.

$$\% \text{ hemolysis} = (ABSs-ABSn)/(ABSp-ABSn) \quad (1)$$

3.2.2.4. Platelet adhesion

Platelet adhesion was evaluated by the methodology proposed by Stahl., et al. [24]. Platelet-rich plasma (PRP) was obtained by spin anticoagulated blood at 120 g for 12 min. Samples with 6 mm in diameter, sterilized by 1 h in UV radiation and stabilized in PBS for 24 h were exposed to PRP (200 µL/sample) at 37 °C for 1 h. Then, samples were washed with PBS to remove any non-adhered platelet on the surface material, and adhered platelets were lysed by soaked samples in 1% triton (200 µL/sample) at 37 °C for 1 h. LDH liberated by adhered platelets on surface material was measured by LDH according to the protocol of CytoTox 96® Non-Radioactive Cytotoxicity Assay kit, measuring absorbance in a iMark Microplate Absorbance Reader (Bio-Rad, Hercules, California, USA) at 490 nm.

3.2.2.5. Protein absorption

The absorption of proteins was evaluated according to Jin et al., [25]. Briefly, samples of 6 mm in diameter, sterilized in UV radiation for 1 h and stabilized in PBS for 24 h were incubated in a solution of bovine serum albumin (BSA) (0.1 µg/mL, 200 µL/sample) for 4 h. Then, each sample was washed three times with PBS and sonicated with 2% SDS solution (200 µL/sample) for 10 min to remove the absorbed proteins. Finally, the concentrations of absorbed proteins by materials were determined by the protocol of Micro BCA™ Protein Assay Kit.

3.2.2.6. Thrombin-Antithrombin complex

Samples (previously sterilized in UV for 1 h and stabilized in PBS for 24 h) located in 2 mL microcentrifuge tubes were exposed to anticoagulated blood (1 mL/sample) at 37 °C for 1 h and centrifuged at 3000 g for 10 min. The concentration of TAT complex in the supernatant was determined according to the protocol of Human Thrombin-Antithrombin Complex ELISA Kit (TAT) indicated by the manufacturer. [23].

3.2.2.7. HUVECS and AoSMC culture

Endothelial and smooth muscle cells were cultured in 75 cm^2 flasks until passage 8 (Figure B1) at 37 °C with 5% CO_2 was accomplished. Then, cells were applied in the assays in passage 9. The medium for cells was changed every 2 days until the flask reached 90% of confluence; at that moment, the passage was carried out.

3.2.2.8. Cell viability

Samples of composite materials of 6 mm in diameter (sterilized in UV radiation for 1 h and stabilized in SmGM-2 culture medium for 24 h) were placed in wells of 96-well plate with a AoSMC suspension of a density of $4x10^5$ cell/mL and incubated at 37 °C with 5% CO_2 for 24 h. An aliquot of 50 µL/sample was taken and deposited in another 96-well plate to measure the LDH released following the protocol of CytoTox 96® Non-Radioactive Cytotoxicity Assay kit [26].

Also, the viability cell of HUVECs was measured in a similar manner. Samples (sterilized in UV radiation for 1 h and stabilized in SmGM-2 culture medium for 24 h) were placed in a

96-well plate with a suspension of cells (150 µL/sample, $1x10^4$ cells/well) at 37 °C with 5% CO_2 for 24 h and the cell viability was obtained following the protocol of CytoTox 96® Non-Radioactive Cytotoxicity Assay kit [14].

The % cell viability was calculated using equation 2.

$$\% \text{ cell viability} = 1 - (ABSs-ABSn)/(ABSp-ABSn) \quad (2)$$

3.2.2.9. Statistics analysis

Assays were made in triplicate. Data were analyzed by an ANOVA of two ways, considering the composition of the matrix (factor 1) and the concentration of the filler (factor 2). Also, polyurethane matrices without fillers were analyzed by an ANOVA of one way. Samples were compere by a post hoc Tukey comparison test. Statical analysis was made in RStudio software version 1.3.1093.

3.3. Results and discussion

Formation of clot is a complex process that when is related with biomaterials is associated with the foreign body response of and the activation of the coagulation cascade. To evaluate the formation of clot caused by composite polyurethanes was conducted the blood clotting time test, showing the results for polyurethane composites without fillers in Figure 3-1 and with AL-N and AL-Z in Table 3-1. These results correspond to the absorbance at 570 nm of hemoglobin, released by lysed red blood cells that were not involved in the clot formation, therefore, at high absorbance values, less development of clot occurred [27]. From Figure 3-1, polyurethane matrix P3 without fillers had the most similar behavior to the control (recalcified blood alone) in comparison with P2 and P1. Also, P3-0%-AL showed less formation of clot at 20 min in a significant degree than P1-0%-AL and P2-0%-AL. This better resistance to the clot formation of P3 in comparison with P1 and P2 matrices could be attributed to the major concentration of PEG, that is reported as an antifouling polymer [28].

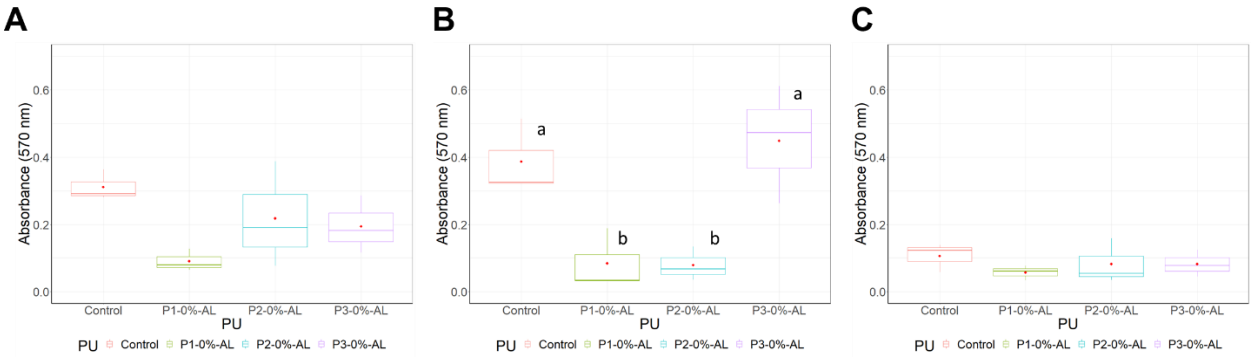

Figure 3-1. *clotting time of exposed recalcified blood to polyurethane matrices without fillers*

Additionally, addition of AL-Z filler showed and improvement of thromboresistance (Table 3-1) in a significant degree for P2-2%-AL-Z compared with P2-0%-AL and P2 with AL-N as a filler at 20 min of the assay. This similar significant difference was identified for P3-2%AL-Z in comparison with P3-0%-AL and composites P3 with AL-N at 20 min and 40 min. These results could be assigned to the increase of hydrophilicity of polyurethane matrix, results reported in the chapter 2, associating this behavior to the reduction of the crystallinity of PEG that improved its chains mobility to the surface [29] and allow the development of a tiny layer of water, which prevents the protein absorption and activation of coagulation cascade [28].

The thrombogenicity characterization of polyurethane composites was conducted according to the ISO 10993-4 to establish the cause of thrombus formation. Between the *in vitro* tests carried out in this work that is proposed by this norm, was evaluated the hemolysis, platelet adhesion, and TAT complex formation (concentration of thrombin). Additionally, protein absorption was studied due to its correlation with the initial stage of clot formation [30].

Results from the hemolysis assay were shown in Figure 3-2. (A) Hemolysis, (B)Platelet adhesion, (C) Protein absorption, and (D) TAT complex caused by polyurethane matrices in the absence of fillersA for polyurethane composites without fillers and in Table 3-2 for composites with AL-N and AL-Z. All materials exhibited a value less than 2% of hemolysis; therefore, these materials are classified as non-hemolytic according to ISO 10993-4. It is important that biomaterials ensure a non-hemolytic property due to lysed red blood cells after its contact with the surface of the material; it could elicit the coagulation cascade by the

release of hemoglobin, which can reduce NO, a compound that activates platelets. Also, hemoglobin can induce the expression of adhesion molecules (ICAM-1 and VCAM-1) presented in endothelial cells, promoting the obstruction of the blood vessel and, consequently, cell damage [31].

Table 3-1. *Clot formation time of recalcified blood in presence of polyurethane composites*

PU	Starch	Concentration	Absorbance at 570 nm		
			t=10 min	**t=20 min**	**t=40 min**
Control			0.32 ± 0.04[a]	0.39 ± 0.11[a]	0.11 ± 0.04[a]
P1	AL-0%		0.09 ± 0.03[a]	0.08 ± 0.09[a]	0.06 ± 0.02[a]
	AL-N	1%	0.13 ± 0.05[a]	0.09 ± 0.06[a]	0.07 ± 0.04[a]
		2%	0.18 ± 0.10[a]	0.08 ± 0.06[a]	0.12 ± 0.06[a]
		3%	0.15 ± 0.09[a]	0.06 ± 0.05[a]	0.04 ± 0.01[a]
	AL-Z	1%	0.24 ± 0.09[a]	0.12 ± 0.05[a]	0.07 ± 0.02[a]
		2%	0.29 ± 0.15[a]	0.07 ± 0.05[a]	0.12 ± 0.05[a]
		3%	0.20 ± 0.05[a]	0.14 ± 0.08[a]	0.11 ± 0.06[a]
P-values					
Starch			0.072	0.450	0.277
Concentration			<0.001*	0.001*	0.047
Starch: Concentration			0.624	0.829	0.417
Control			0.32 ± 0.04[a]	0.39 ± 0.11[ace]	0.11 ± 0.04[abc]
P2	AL-0%		0.22 ± 0.16[a]	0.08 ± 0.05[be]	0.08 ± 0.07[ac]
	AL-N	1%	0.14 ± 0.04[a]	0.08 ± 0.03[bce]	0.04 ± 0.01[a]
		2%	0.27 ± 0.08[a]	0.05 ± 0.02[be]	0.06 ± 0.01[ab]
		3%	0.19 ± 0.09[a]	0.10 ± 0.06[bce]	0.08 ± 0.02[abc]
	AL-Z	1%	0.24 ± 0.09[a]	0.07 ± 0.02[be]	0.05 ± 0.01[a]
		2%	0.33 ± 0.15[a]	0.31 ± 0.17[ce]	0.26 ± 0.06[bc]
		3%	0.23 ± 0.14[a]	0.15 ± 0.04[e]	0.23 ± 0.06[c]
P-values					
Starch			0.362	0.022*	0.004*
Concentration			0.207	<0.001*	0.002*
Starch: Concentration			0.832	0.011*	0.036*
Control			0.32 ± 0.04[a]	0.39 ± 0.11[a]	0.11 ± 0.04[abcd]
P3	AL-0%		0.19 ± 0.08[a]	0.45 ± 0.17[a]	0.08 ± 0.04[acd]
	AL-N	1%	0.25 ± 0.11[a]	0.33 ± 0.14[a]	0.10 ± 0.03[abcd]
		2%	0.16 ± 0.057[a]	0.31 ± 0.16[a]	0.09 ± 0.06[acd]
		3%	0.16 ± 0.07[a]	0.20 ± 0.04[a]	0.12 ± 0.04[abcd]
	AL-Z	1%	0.24 ± 0.07[a]	0.22 ± 0.12[a]	0.28 ± 0.08[bd]
		2%	0.27 ± 0.01[a]	0.20 ± 0.07[a]	0.21 ± 0.04[cd]
		3%	0.28 ± 0.03[a]	0.23 ± 0.02[a]	0.19 ± 0.04[d]
P-values					
Starch			0.064	0.407	0.005*
Concentration			0.091	0.019*	0.038*
Starch: Concentration			0.231	0.676	0.122

**Samples with the same letter do not have a statistically significant difference. Samples with a different letter have significant differences.
*Effects statistically significant (p-value < 0.05)

Activation and adhesion of platelets is the assay most used to characterize the antithrombotic property of biomaterials due to its direct correlation with the formation of the clot. Platelet activation conduces to a platelet aggregation which forms a platform that contains phospholipids (compound presented in the structure of platelets) related with the elicit of the activation of factor X from the coagulation cascade, causing the activation of other factors that results in the production of fibrin (principal polymer of clots) [9]. Platelet adhesion on composites polyurethanes was evaluated by the release of LDH from lysed platelets adhered to the surface of composites. Results reported for polyurethane matrices without fillers (Figure 3-2B) and composites with AL-N or AL-Z (Table 3-2) correspond to the absorbance of LDH at 450 nm; therefore, higher values of absorbance are associated with major platelet adhesion. From Figure 3-2B was observed that polyurethane matrices without fillers had no significant difference with biomaterial from GORE® PROPATEN® Vascular Graft, which contains heparin at the surface, a compound characterized as an antithrombotic agent [32]. Also, the addition of fillers (AL-N or AL-Z) did not exhibit any significant difference (Table 3-2). These results are consistent with the literature reported for materials that contain PEG, which attributes the resistance to platelet adhesion to the water layer bounded around hydrophilic groups of this polymer [33,34].

Certain protein absorption in biomaterials (especially fibrinogen) is associated with the activation of the intrinsic pathway of the coagulation cascade, complement system, and immunology response (activation of neutrophils and macrophages) [8]. However, some investigations [35-37] have reported that selective adsorption of albumin, which is the major protein in the human blood plasma [38], reduces the adhesion of platelets due to this protein does not have an amino acid sequence that binds with activation receptor of platelets [30], for this reason, it is important the measurement of the absorption of this molecule by polyurethane composites. Protein absorption by polyurethane matrices in the absence of fillers (Figure 3-2C) showed that P2 and P3 had the largest value in a significant degree when compared with P1. This phenomenon could be due to electrostatic interactions between PEG segment and albumin, which is analogous to the phenomena reported by Bremmell., et al. [35], who studied the electrostatic effect in albumin adsorption on modified surface of silicon

with PEG-CHO and PEG-SO_3, finding that PEG-SO_3 absorbed albumin at high ionic strength, related with the interaction of cationic sides of this protein (which has an overall negative charge) with ionic surfaces. The inclusion of filler (AL-N or AL-Z) in polyurethane matrices did not have any significant difference in the protein adsorption (Table 3-2).

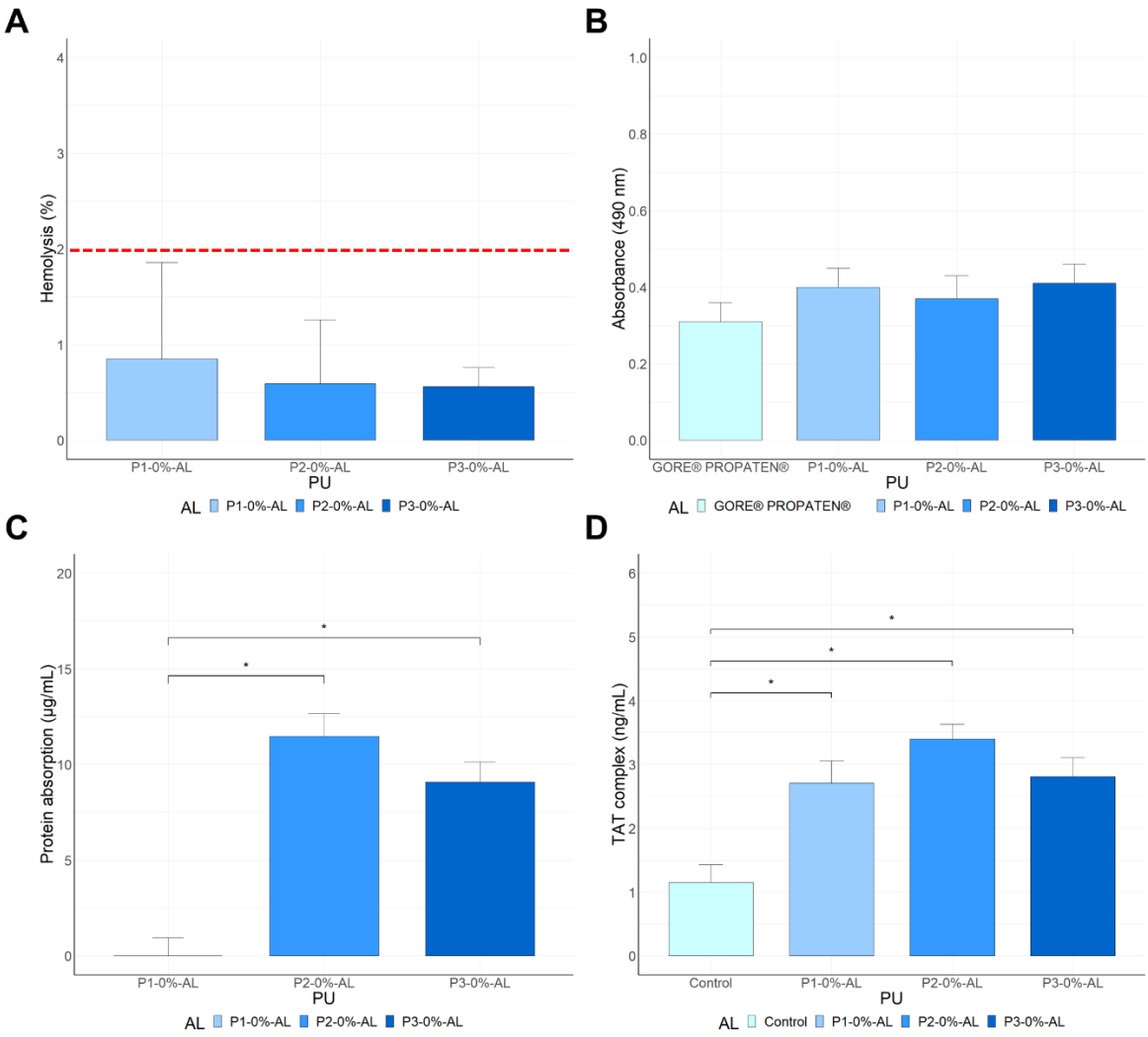

Figure 3-2. *(A) Hemolysis, (B)Platelet adhesion, (C) Protein absorption, and (D) TAT complex caused by polyurethane matrices in the absence of fillers*

Table 3-2. *Blood-composites contact assays*

PU	Starch	Concentration	Hemolysis (%)	Platelet adhesion (absorbance)	Protein absorption (μg/mL)	TAT complex (ng/mL)
Control			-	0.31 ± 0.05^{a}	-	1.15 ± 0.28^{acde}
P1	AL-N	AL-0%	0.84 ± 1.01^{a}	0.39 ± 0.04^{a}	0.00 ± 0.94^{a}	2.71 ± 0.34^{b}
		1%	0.35 ± 0.32^{a}	0.42 ± 0.17^{a}	0.00 ± 0.53^{a}	3.12 ± 0.38^{b}
		2%	0.47 ± 0.60^{a}	0.38 ± 0.04^{a}	0.00 ± 1.05^{a}	3.13 ± 0.38^{b}
		3%	1.02 ± 0.36^{a}	0.38 ± 0.05^{a}	0.00 ± 0.34^{a}	2.99 ± 0.25^{b}
	AL-Z	1%	0.32 ± 0.56^{a}	0.37 ± 0.09^{a}	0.00 ± 0.34^{a}	1.81 ± 0.26^{c}
		2%	0.18 ± 0.15^{a}	0.32 ± 0.04^{a}	0.00 ± 0.37^{a}	1.66 ± 0.25^{d}
		3%	0.38 ± 0.66^{a}	0.37 ± 0.04^{a}	0.00 ± 0.52^{a}	1.55 ± 0.19^{e}
P-values						
Starch			0.379	0.379	0.573	<0.001*
Concentration			0.425	0.166	0.998	<0.001*
Starch : Concentration			0.815	0.908	0.680	<0.001*
Control			-	0.31 ± 0.05^{a}	-	1.15 ± 0.28^{ac}
P2	AL-N	AL-0%	0.58 ± 0.67^{a}	0.37 ± 0.06^{a}	11.46 ± 1.20^{ab}	3.40 ± 0.23^{b}
		1%	0.20 ± 0.35^{a}	0.38 ± 0.07^{a}	13.44 ± 1.10^{ab}	2.00 ± 1.13^{c}
		2%	0.14 ± 0.25^{a}	0.40 ± 0.05^{a}	12.76 ± 1.91^{ab}	1.35 ± 0.28^{c}
		3%	0.76 ± 0.66^{a}	0.49 ± 0.12^{a}	15.55 ± 2.78^{a}	1.19 ± 0.12^{c}
	AL-Z	1%	0.20 ± 0.35^{a}	0.36 ± 0.06^{a}	11.89 ± 2.90^{ab}	1.36 ± 0.40^{c}
		2%	0.55 ± 0.96^{a}	0.34 ± 0.05^{a}	7.86 ± 2.46^{b}	1.28 ± 0.26^{c}
		3%	0.32 ± 0.56^{a}	0.31 ± 0.04^{a}	12.95 ± 3.71^{ab}	1.21 ± 0.21^{c}
P-values						
Starch			0.977	0.035*	0.031*	0.437
Concentration			0.677	0.242	0.055	<0.001*
Starch : Concentration			0.688	0.124	0.356	0.757
Control			-	0.31 ± 0.05^{ab}	-	1.15 ± 0.28^{ac}
P3	AL-N	AL-0%	0.55 ± 0.20^{a}	0.41 ± 0.05^{ab}	9.08 ± 1.06^{a}	2.81 ± 0.30^{b}
		1%	0.32 ± 0.20^{a}	0.40 ± 0.06^{ab}	10.92 ± 2.41^{a}	1.58 ± 0.89^{c}
		2%	0.79 ± 0.18^{a}	0.44 ± 0.06^{ab}	13.87 ± 2.89^{a}	1.04 ± 0.02^{c}
		3%	0.26 ± 0.30^{a}	0.48 ± 0.06^{a}	15.17 ± 3.47^{a}	1.03 ± 0.08^{c}
	AL-Z	1%	0.57 ± 0.27^{a}	0.31 ± 0.06^{ab}	12.43 ± 1.32^{a}	1.16 ± 0.02^{c}
		2%	0.35 ± 0.53^{a}	0.30 ± 0.05^{b}	11.46 ± 5.94^{a}	1.10 ± 0.24^{c}
		3%	0.57 ± 0.36^{a}	0.32 ± 0.05^{ab}	13.14 ± 4.31^{a}	1.09 ± 0.11^{c}
P-values						
Starch			0.862	<0.001*	0.588	0.755
Concentration			0.734	0.048*	0.088	<0.001
Starch : Concentration			0.188	0.054	0.701	0.844

**Samples with the same letter do not have a statistically significant difference. Samples with a different letter have significant differences.
*Effects statistically significant (p-value < 0.05)

The formation of thrombin is a crucial step in the coagulation cascade due to this enzyme converts the fibrinogen to fibrin (polymer that compound the clot) [9]. Therefore, the concentration of thrombin was evaluated in this study by the TAT complex assay. From Figure 3-2D was noted that polyurethane matrices without fillers increase by a significant degree the concentration of thrombin in comparison with the control (anticoagulated fresh blood alone). From Table 3-2, the addition of fillers reduced to a significant degree the concentration of thrombin; especially, the inclusion of AL-Z at the highest concentration (3% wt) reduced the TAT complex until it was like the control. These results could be attributed to the increase of mobility chains of soft segments, principally of PEG segment, due to the reduction of soft domains crystallinity as was reported in the chapter 2. That reduction of crystallinity allows better hydrophilicity of the surface and the formation of a water barrier that could reduce the activation of factor XII.

The evaluation of biocompatibility of composite polyurethanes was conducted by the exposition of HUVECs and AoSMC to composites, determining its cells viability. It is well known that the proliferation of adherent cells depends on their attachment to a surface; otherwise, cells can suffer apoptosis. From Table 3-3 was noted that polyurethane matrices without fillers did not exhibit any significant difference for viability of both cells. Additionally, addition of fillers (AL-N or AL-Z) reduces the HUVECs viability for P2 and P3 composites polyurethanes in a significant degree compared with its respective polyurethane matrices without fillers. This reduction is major when AL-Z was used as a filler in comparison with AL-N. These results could be attributed to an increase of hydrophilicity of surfaces which reduces the cell adhesion and, therefore, its capacity to proliferate [22]. Likewise, the inclusion of AL-Z in the P1 polyurethane matrix increased the cell viability of AoSMC. The surface of P1 was more hydrophobic (contact angle between 103.7–110.3°) compared with the other matrices (99.5–39.4°). This suggested that the surface requirements for HUVECs and AoSMCs adhesion are different, and it is of interest in the design of cardiovascular applications.

Table 3-3. *HUVECs and AoSMC viability in presence of polyurethane composites*

PU	Starch	Concentration	HUVECs viability (%)	AoSMC viability (%)
	Control		100%	100%
		AL-0%	82.23 ± 0.96[a]	106.59 ± 17.02[a]
		1%	88.28 ± 4.57[a]	99.73 ± 4.15[a]
	AL-N	2%	89.74 ± 2.74[a]	106.73 ± 3.08[a]
P1		3%	92.49 ± 3.09[a]	105.14 ± 4.72[a]
		1%	85.98 ± 4.00[a]	195.23 ± 22.38[b]
	AL-Z	2%	83. 79 ± 9.29[a]	172.40 ± 37.82[b]
		3%	88.73 ± 2.48[a]	195.10 ± 14.20[b]
	P-values			
	Starch		0.107	<0.001*
	Concentration		0.031*	0.003*
	Starch : Concentration		0.683	0.001*
	Control		100%	100%
		AL-0%	83.24 ± 3.96[a]	100.26 ± 2.39[a]
		1%	71.70 ± 21.26[ab]	105.80 ± 5.38[a]
	AL-N	2%	79.94 ± 11.29[a]	98.65 ± 16.79[a]
P2		3%	64.74 ± 12.67[ab]	83.72 ± 33.96[a]
		1%	37.91 ± 10.28[b]	169.49 ± 58.56[a]
	AL-Z	2%	33.70 ± 11.82[b]	141.18 ± 18.07[a]
		3%	34.89 ± 22.37[b]	166.05 ± 46.96[a]
	P-values			
	Starch		<0.001*	0.002*
	Concentration		0.003*	0.239
	Starch : Concentration		0.059	0.152
	Control		100%	100%
		AL-0%	77.01 ± 9.35[a]	81.79 ± 20.28[a]
		1%	77.93 ± 5.21[a]	78.13 ± 9.05[a]
	AL-N	2%	69.78 ± 11.13[ac]	75.03 ± 15.91[a]
P3		3%	79.12 ± 6.19[a]	71.68 ± 36.78[a]
		1%	35.44 ± 6.71[bc]	79.06 ± 43.76[a]
	AL-Z	2%	40.11 ± 14.60[bc]	115.04 ± 54.41[a]
		3%	45.78 ± 7.41[c]	112.08 ± 22.78[a]
	P-values			
	Starch		<0.001*	0.133
	Concentration		0.003*	0.771
	Starch : Concentration		0.006*	0.512

**Samples with the same letter do not have a statistically significant difference. Samples with a different letter have significant differences.
*Effects statistically significant (p-value < 0.05

3.4. Conclusions

The synthesis of composite polyurethanes was confirmed by ATR-FTIR and SEM. Also, the anti-thrombogenic activity of the materials was characterized by the blood clotting time. The cause of thrombus formation was studied according to ISO 10993-4, evaluating the hemolysis, platelet adhesion, and TAT complex. These assays were complemented with the development of the protein adsorption assay and HUVECs and AoSMC viability assay. Blood clotting time assay showed that polyurethane matrix P3 without fillers has a better thromboresistance property in comparison with P1 and P2. Also, the hemolysis assay exhibit that all materials are not hemolytic. From platelet adhesion assay, all materials have similar behavior in comparison with heparin-modified commercial graft. Protein absorption results showed that polyurethane matrices P2 and P3 had adsorption of albumin; however, it is necessary to evaluate the Vroman effect with a blending of proteins to establish the behavior of protein absorption from materials. According to TAT complex assay, AL-Z improves the resistance to thrombus formation due to the reduction of thrombin concentration. Finally, the cell viability assay evaluated with HUVECs and AoSMC exhibited that composite polyurethanes P1 could be classified as inert materials in the context of cardiovascular applications

3.5. References

1. Mastroiacovo G, Guarino A, Pirola S, Gennari M, Capriuoli F, Micheli B, et al. Cardiovascular tissue banking activity during SARS-CoV-2 pandemic: evolution of national protocols and Lombardy experience. Cell Tissue Bank [Internet]. 2021;22(4), :675–683. Available from: https://doi.org/10.1007/s10561-021-09959-z

2. Montaña Chaparro WF, Díaz Roa KA, Otálvaro Cifuentes EH. Situación actual de los bancos de tejidos en Colombia: tejido cardiovascular. Rev Colomb Cardiol [Internet]. 2019. ; Available from: http://www.sciencedirect.com/science/article/pii/S0120563319300397

3. Obiweluozor FO, Emechebe GA, Kim DW, Cho HJ, Park CH, Kim CS, et al. Considerations in the Development of Small-Diameter Vascular Graft as an Alternative for Bypass and Reconstructive Surgeries: A Review. Cardiovasc Eng Technol. 2020;11(5), :495–521.

4. Montrief T, Koyfman A, Long B. Coronary artery bypass graft surgery complications: A review for emergency clinicians. Am J Emerg Med [Internet]. 2018;36(12), :2289–2297. Available from: https://doi.org/10.1016/j.ajem.2018.09.014

5. Sung YK, Lee DR, Chung DJ. Advances in the development of hemostatic biomaterials for medical application. Biomater Res. 2021;25(1), :1–10.

6. Horbett TA. Selected aspects of the state of the art in biomaterials for cardiovascular applications. Colloids Surfaces B Biointerfaces. 2020;191, 110986.

7. Labarrere CA, Dabiri AE, Kassab GS. Thrombogenic and Inflammatory Reactions to Biomaterials in Medical Devices. Front Bioeng Biotechnol. 2020;8. doi: 10.3389/fbioe.2020.00123.

8. Horbett TA. Adsorbed Proteins on Biomaterials. Biomater Sci An Introd to Mater Third Ed. 2013;394–408.

9. Hanson SR, Tucker EI. Blood Coagulation and Blood - Materials Interactions. Biomater Sci An Introd to Mater Third Ed. 2013;(1997), :551–557.

10. Anderson JM. Inflammation, Wound Healing, and the Foreign-Body Response. Biomater Sci An Introd to Mater Third Ed. 2013;(2005), :503–512.

11. Lavery KS, Rhodes C, Mcgraw A, Eppihimer MJ. Anti-thrombotic technologies for medical devices. Adv Drug Deliv Rev [Internet]. 2017;112, :2–11. Available from: http://dx.doi.org/10.1016/j.addr.2016.07.008

12. Gostev AA, Karpenko AA, Laktionov PP. Polyurethanes in cardiovascular prosthetics. Polym Bull [Internet]. 2018;75(9), :4311–4325. Available from: https://doi.org/10.1007/s00289-017-2266-x

13. Roth Y, Lewitus DY. The grafting of multifunctional antithrombogenic chemical networks on polyurethane intravascular catheters. Polymers (Basel). 2020;12(5), 1131.

14. Xu C, Kuriakose AE, Truong D, Punnakitikashem P, Nguyen KT, Hong Y. Enhancing anti-thrombogenicity of biodegradable polyurethanes through drug molecule incorporation. J Mater Chem B. 2018;6(44), :7288–7297.

15. Ye SH, Hong Y, Sakaguchi H, Shankarraman V, Luketich SK, DAmore A, et al. Nonthrombogenic, biodegradable elastomeric polyurethanes with variable sulfobetaine content. ACS Appl Mater Interfaces. 2014;6(24), :22796–22806.

16. Tazawa S, Maeda T, Nakayama M, Hotta A. Synthesis of Thermoplastic Poly(2-methoxyethyl acrylate)-Based Polyurethane by RAFT and Condensation Polymerization. Macromol Rapid Commun. 2020;41(19), :1–5.

17. Chen X, Gu H, Lyu Z, Liu X, Wang L, Chen H, et al. Sulfonate Groups and Saccharides as Essential Structural Elements in Heparin-Mimicking Polymers Used as Surface Modifiers: Optimization of Relative Contents for Antithrombogenic Properties. ACS Appl Mater Interfaces. 2018;10(1), :1440–1449.

18. Liu P, Huang T, Liu P, Shi S, Chen Q, Li L, et al. Zwitterionic modification of polyurethane membranes for enhancing the anti-fouling property. J Colloid Interface Sci [Internet]. 2016;480, :91–101. Available from: http://www.sciencedirect.com/science/article/pii/S0021979716304568

19. Arévalo F, Uscategui YL, Diaz L, Cobo M, Valero MF. Effect of the incorporation of chitosan on the physico-chemical, mechanical properties and biological activity on a mixture of polycaprolactone and polyurethanes obtained from castor oil. J Biomater Appl. 2016;31(5), :708–720.

20. De Mel A, Chaloupka K, Malam Y, Darbyshire A, Cousins B, Seifalian AM. A silver nanocomposite biomaterial for blood-contacting implants. J Biomed Mater Res - Part A. 2012;100 A(9), :2348–2357.

21. Erathodiyil N, Chan H-M, Wu H, Ying JY. Zwitterionic polymers and hydrogels for antibiofouling applications in implantable devices. Mater Today [Internet]. 2020;38, :84–98. Available from: http://www.sciencedirect.com/science/article/pii/S1369702120301012

22. Wang J, Sun H, Li J, Dong D, Zhang Y, Yao F. Ionic starch-based hydrogels for the prevention of nonspecific protein adsorption. Carbohydr Polym. 2015;117, :384–391.

23. Punnakitikashem P, Truong D, Menon JU, Nguyen KT, Hong Y. Electrospun biodegradable elastic polyurethane scaffolds with dipyridamole release for small diameter vascular grafts. Acta Biomater [Internet]. 2014;10(11), :4618–4628. Available from: http://dx.doi.org/10.1016/j.actbio.2014.07.031

24. Stahl AM, Yang YP. Tunable Elastomers with an Antithrombotic Component for Cardiovascular Applications. Adv Healthc Mater. 2018;7(16), :1–10.

25. Jin Y, Zhu Z, Liang L, Lan K, Zheng Q, Wang Y, et al. A facile heparin/carboxymethyl chitosan coating mediated by polydopamine on implants for hemocompatibility and antibacterial properties. Appl Surf Sci [Internet]. 2020;528,

:146539.

26. Morales-Gonzalez M, Arévalo-Alquichire S, Diaz LE, Sans JÁ, Vilarinõ-Feltrer G, Gómez-Tejedor JA, et al. Hydrolytic stability and biocompatibility on smooth muscle cells of polyethylene glycol-polycaprolactone-based polyurethanes. J Mater Res. 2020;35(23–24), :3276–3285.

27. Dey J, Xu H, Nguyen KT, Yang J. Crosslinked urethane doped polyester biphasic scaffolds: Potential for in vivo vascular tissue engineering. J Biomed Mater Res - Part A. 2010;95 A(2), :361–370.

28. Adipurnama I, Yang M-C, Ciach T, Butruk-Raszeja B. Surface modification and endothelialization of polyurethane for vascular tissue engineering applications: A review. Biomater Sci. 2017;5(1), :22–37.

29. Kumar S, Tewatia P, Samota S, Rattan G, Kaushik A. Ameliorating properties of castor oil based polyurethane hybrid nanocomposites via synergistic addition of graphene and cellulose nanofibers. J Ind Eng Chem [Internet]. 2022;109, :492–509. Available from: https://doi.org/10.1016/j.jiec.2022.02.035

30. Brash JL, Horbett TA, Latour RA, Tengvall P. The blood compatibility challenge. Part 2: Protein adsorption phenomena governing blood reactivity. Acta Biomater [Internet]. 2019;94, :11–24. Available from: https://doi.org/10.1016/j.actbio.2019.06.022

31. Braune S, Latour RA, Reinthaler M, Landmesser U, Lendlein A, Jung F. In Vitro Thrombogenicity Testing of Biomaterials. Adv Healthc Mater. 2019;8(21), 1900527.

32. Drozd NN, Lunkov AP, Shagdarova BT, Zhuikova Y V., Il'ina A V., Varlamov VP. Thromboresistance of Polyurethane Plates Modified with Quaternized Chitosan and Heparin. Appl Biochem Microbiol. 2022;58(3), :315–21.

33. Vakili H, Mohseni M, Ghanbari H, Yahyaei H, Makki H, González A, et al. Enhanced hemocompatibility of a PEGilated polycarbonate based segmented polyurethane. Int J Polym Mater Polym Biomater [Internet]. 2022;71(7), :531–539.

Available from: https://doi.org/10.1080/00914037.2020.1857760

34. Wang Y, Ma B, Liu K, Luo R, Wang Y. A multi-in-one strategy with glucose-triggered long-term antithrombogenicity and sequentially enhanced endothelialization for biological valve leaflets. Biomaterials [Internet]. 2021;275(June), :120981. Available from: https://doi.org/10.1016/j.biomaterials.2021.120981

35. Bremmell KE, Britcher L, Griesser HJ. Steric and electrostatic surface forces on sulfonated PEG graft surfaces with selective albumin adsorption. Colloids Surfaces B Biointerfaces [Internet]. 2013;106, :102–108. Available from: http://dx.doi.org/10.1016/j.colsurfb.2013.01.052

36. Fedel M, Motta A, Maniglio D, Migliaresi C. Surface properties and blood compatibility of commercially available diamond-like carbon coatings for cardiovascular devices. J Biomed Mater Res - Part B Appl Biomater. 2009;90 B(1), :338–349.

37. Kottke-Marchant K, Anderson JM, Umemura Y, Marchant RE. Effect of albumin coating on the in vitro blood compatibility of Dacron® arterial prostheses. Biomaterials. 1989;10(3), :147–155.

38. Mishra V, Heath RJ. Structural and biochemical features of human serum albumin essential for eukaryotic cell culture. Int J Mol Sci. 2021;22(16), 8411.

4. Conclusions

The study of physicochemical, mechanical, and thermal properties of polyurethane composites identified that adding filler modified in a significant degree the physicochemical and mechanical properties. The addition of AL-N and AL-Z in polyurethane matrices changed the order of soft domain chains, reducing the crystallinity degree of PEG and PCL segments, especially, in P1 composition matrix. This reduction of the order affected the surface and bulk properties of matrices, increasing its hydrophilicity (principally for P3) which is related to an improvement of antifouling behavior, a property required for cardiovascular applications.

Additionally, the inclusion of fillers affected the mechanical properties of polyurethane matrices. The inclusion of AL-N improves tensile strength in P1 compositions. However, for concentrations large than 1%, this property was negatively affected due to the formation of agglomerates. On the other hand, AL-Z reduced mechanical properties in all polyurethane matrices. Despite these results, all composite polyurethanes exhibited values of tensile strength above 1 MPa, which is the tensile strength of the femoral artery (autologous graft used in CABPG).

Evaluation of antithrombogenicity activity permitted us to find that the addition of fillers, especially AL-Z, increases the thrombogenic resistance of polyurethane matrices due to the reduction in the concentration of thrombin. These results established that the thrombogenicity activity of these materials is related to the activation of the cascade of coagulation. For this reason, *in vitro* studies suggest that materials could be applied in cardiovascular applications, considering that fillers increase the hydrophilicity property, maintain tensile strength above 1 MPa and reduce the concentration of thrombin.

5. Perspectives and recommendations

From this work was observed that synthetic materials used for blood contact applications could activate the intrinsic coagulation cascade from the evaluation of TAT complex. For a better understanding of the phenomena of clot formation associated with polyurethane composites obtained in this research, it could be established that future studies should focus their efforts on evaluating the activation of complement and immunologic systems from these composites due to these responses are related to the inflammation of adjacent tissue, in the anastomosis site, conducing to intima hyperplasia.

Also, to understand in a better form the Vroman effect, which is related to the adsorption of proteins at surface materials, *in vivo* studies should conduct in future research that allows establishing in a solid base the body response in front of these materials.

6. **Appendix A.** Supplementary material of Influence of starch on the structure-properties relationship in polyethylene glycol/polycaprolactone diol polyurethanes

Figure A 1. *Synthesis of zwitterionic starch after (A) twelve-hour of reaction, (B) neutralization, precipitation, and three wash with methanol, (C) smash in methanol, and (D) filtration.*

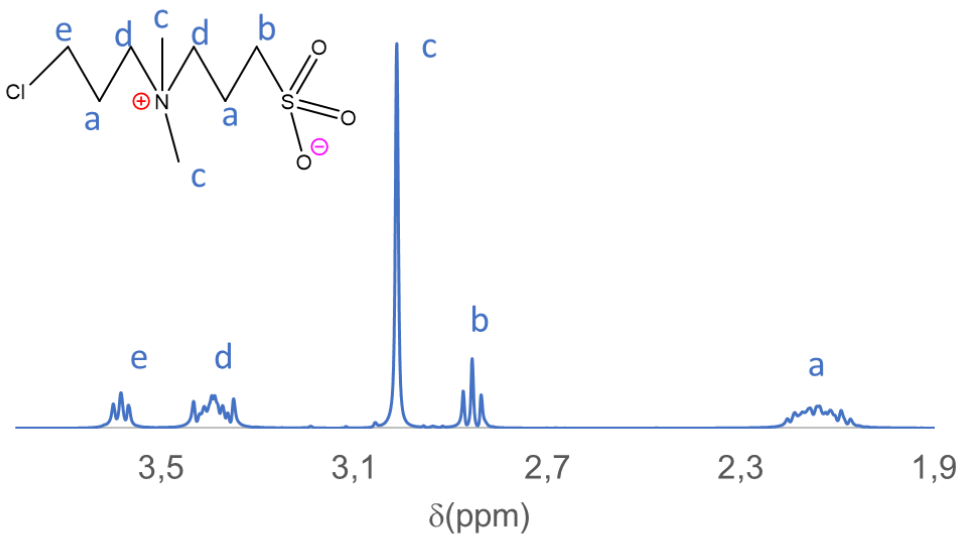

Figure A 2. *^{1}H RMN spectrum of DCAPS*

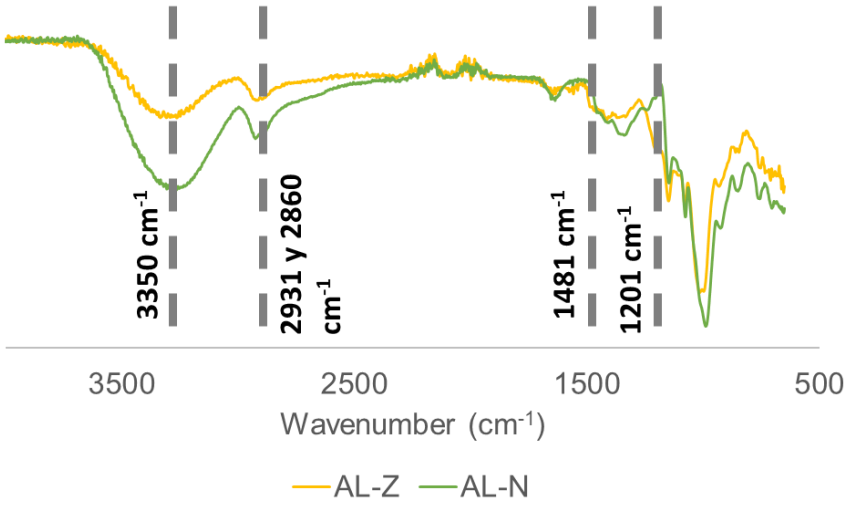

Figure A 3. *FTIR spectra of AL-N and AL-Z*

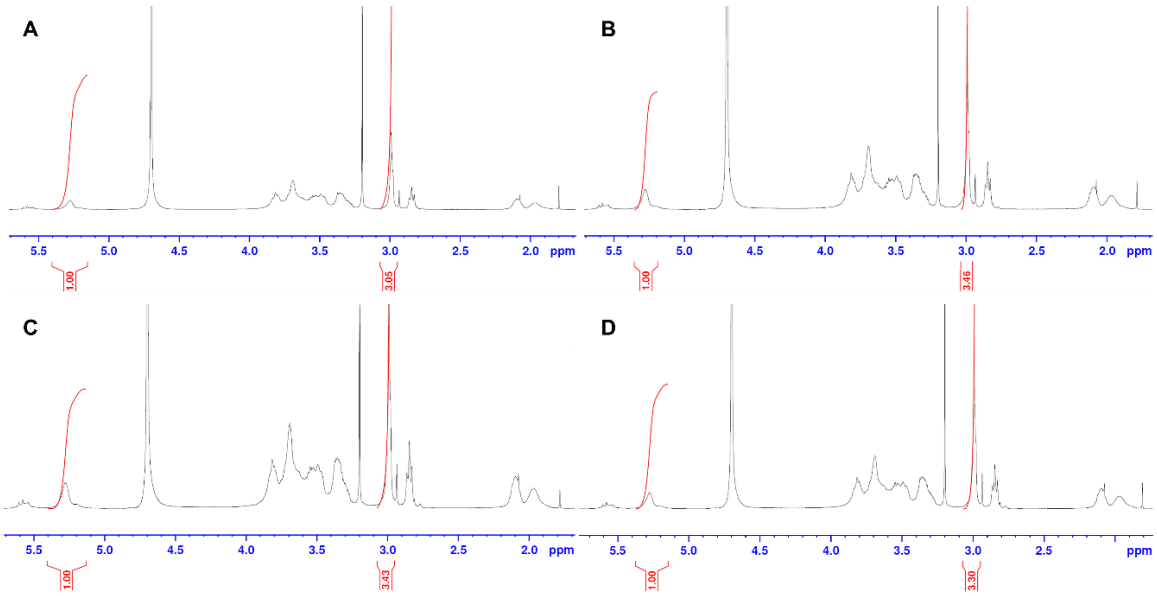

Figure A 4. *AL-Z synthesis replicate (A) 1, (B) 2, (C) 3, and (D) 4*

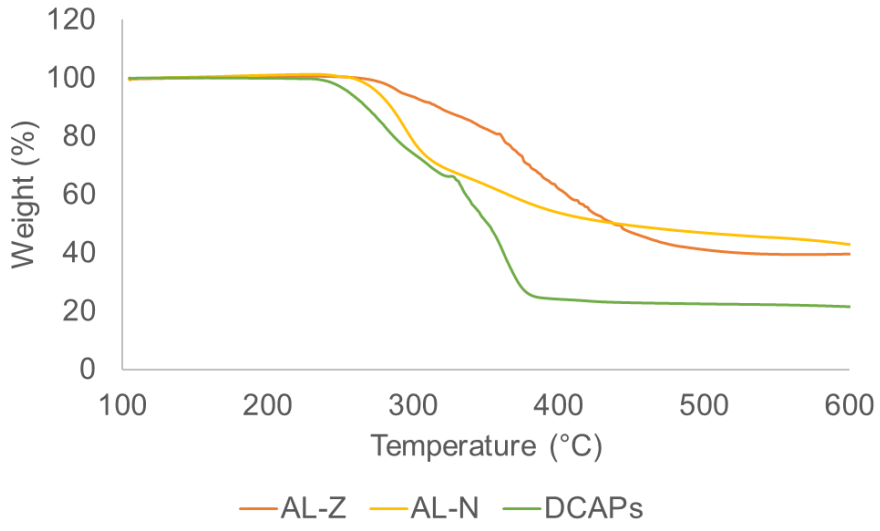

Figure A 5*. TGA of AL-N, AL-Z and DCPAS*

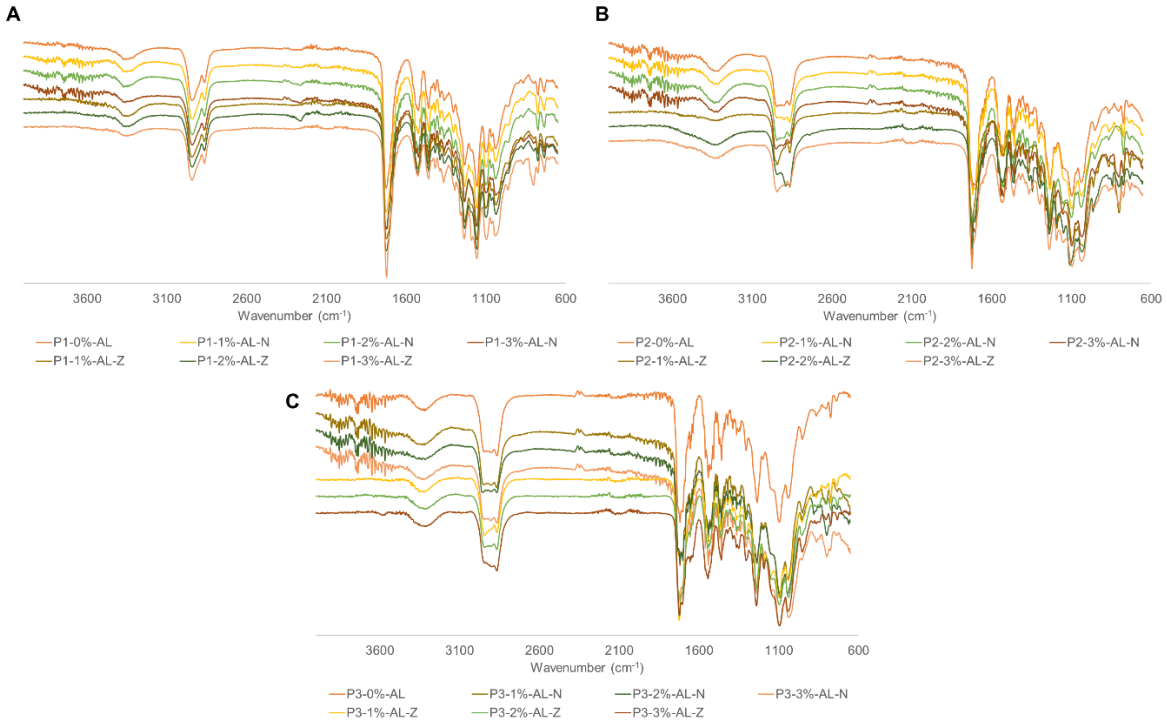

Figure A 6. *FTIR spectra of (A) P1, (B) P2, and (C) P3 of polyurethane composites*

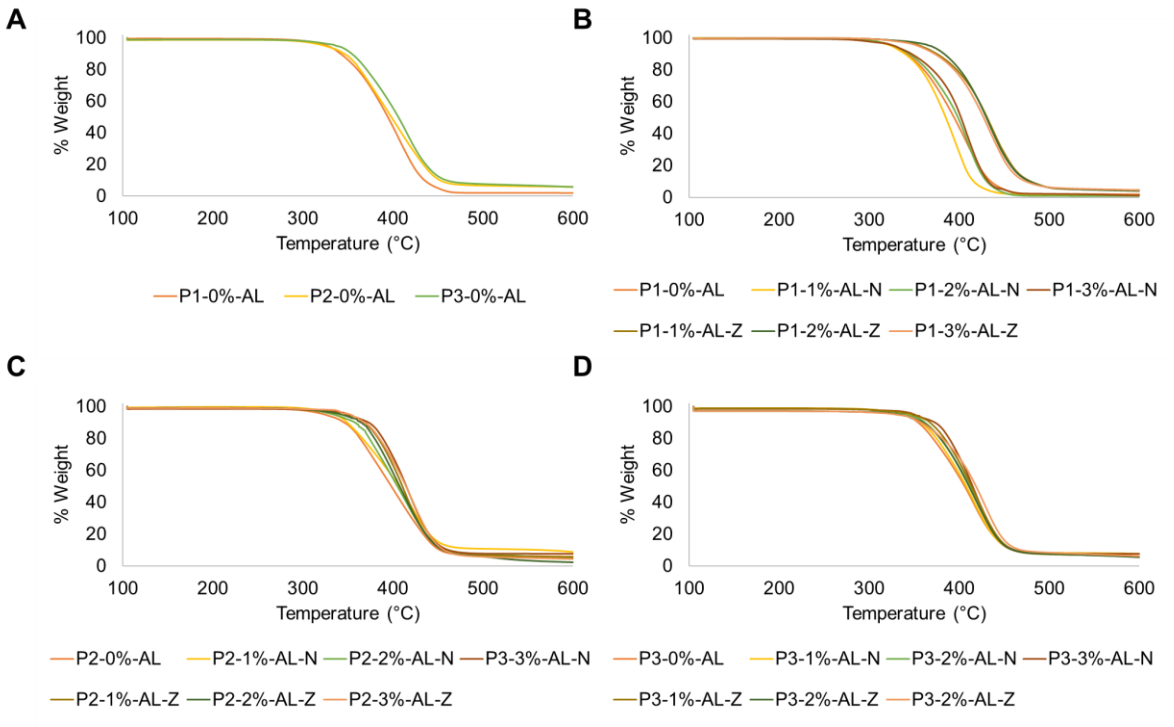

Figure A 7. *TGA of polyurethane (A) without fillers, (B) P1, (C) P2, and (D) P3 composites*

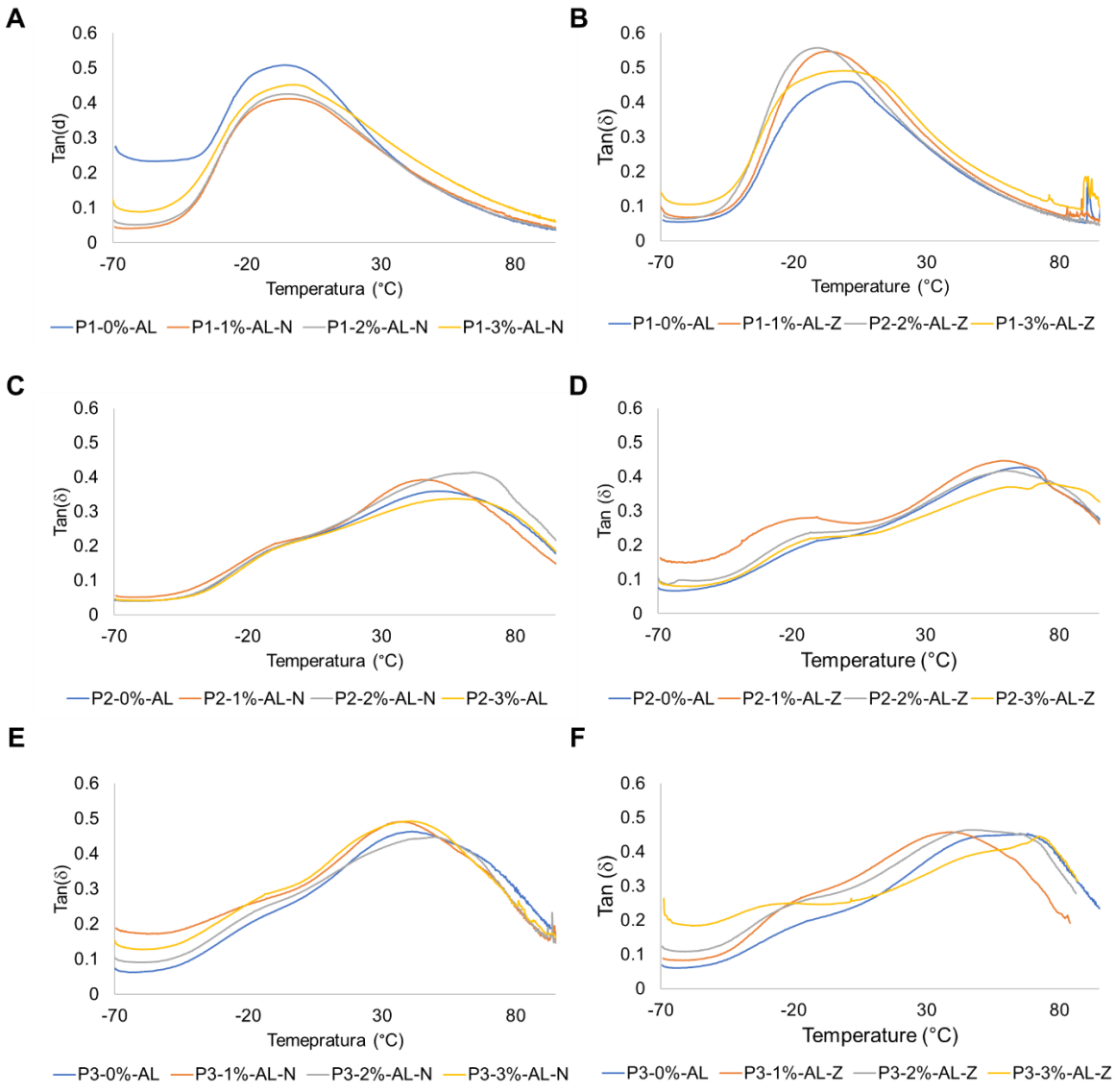

Figure A 8. *Loss factor of composite polyurethane P1 (A-B), P2 (C-D), and P3 (E-F)*

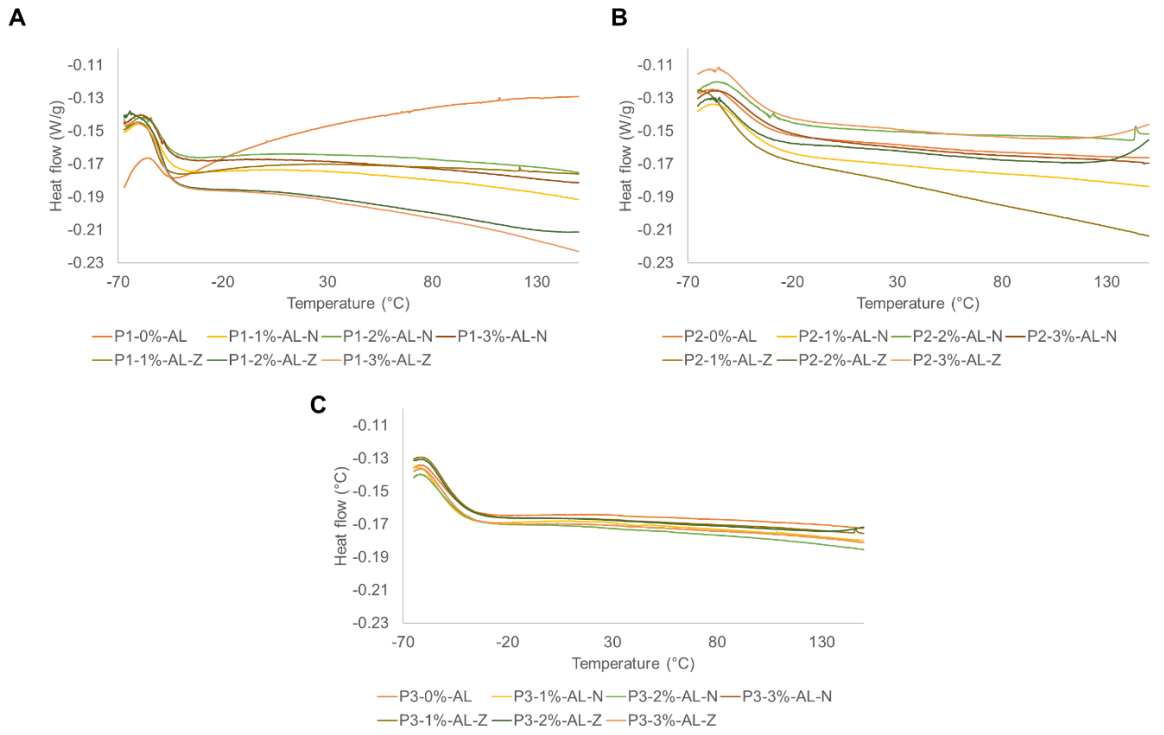

Figure A 9. *DSC of polyurethane (A) P1, (B) P2, and (C) P3 composites*

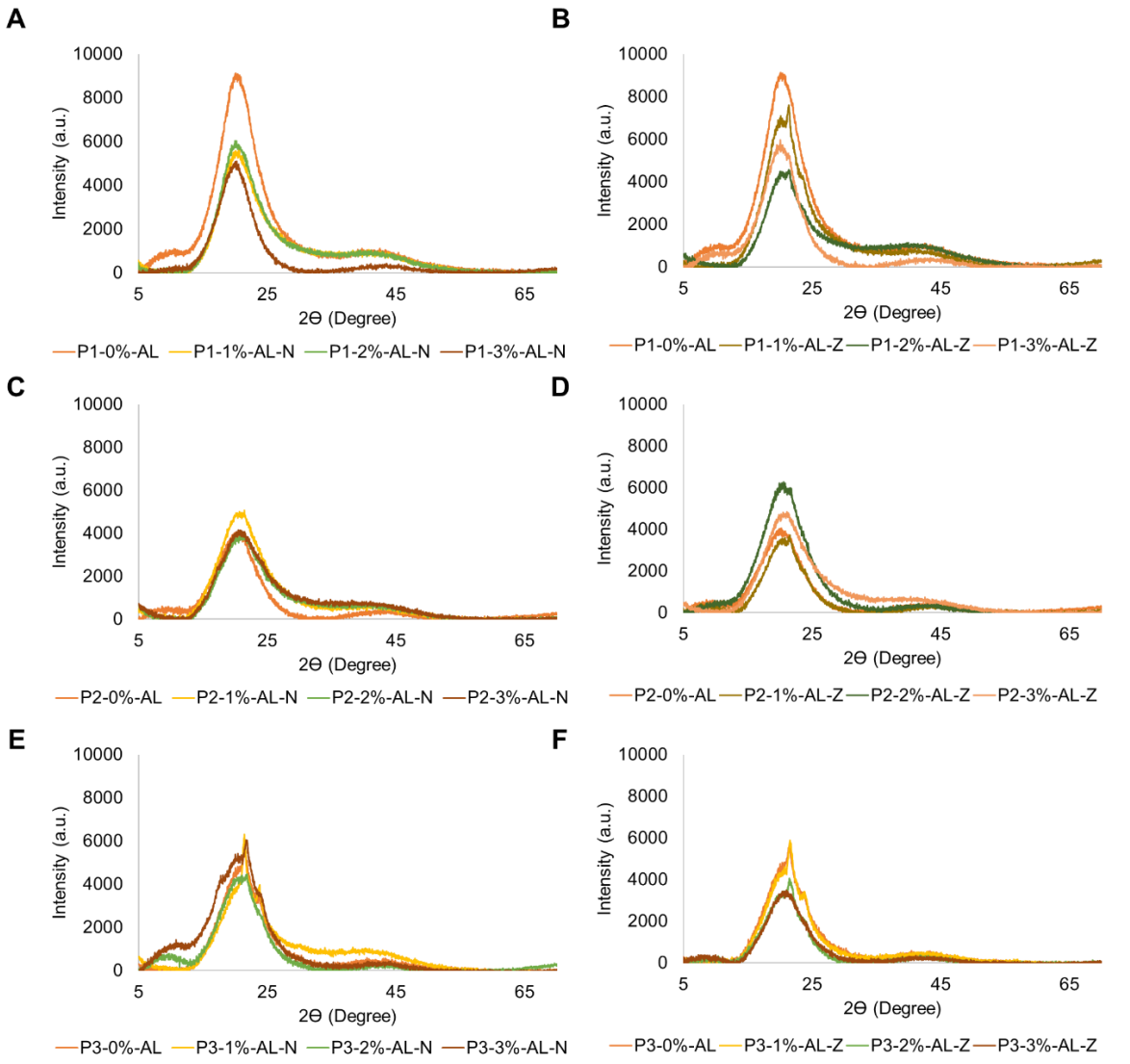

Figure A 10. *XRD spectra of composite polyurethane P1 (A-B), P2 (C-D), and P3 (E-F)*

7. **Appendix B.** Supplementary material of Assessment of the anti-thrombogenic activity of polyurethane starch composites

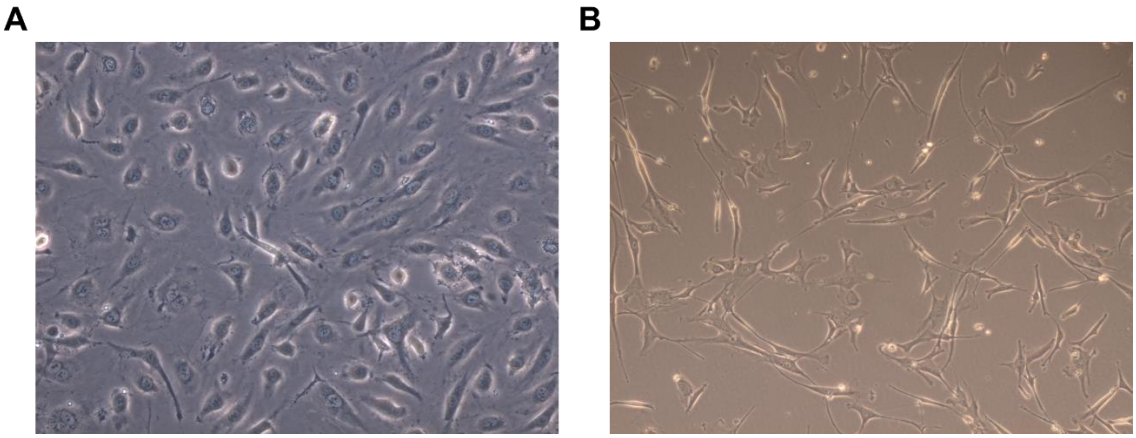

Figure B1. *Cell culture in passage 8 of (A) HUVECs, and (B) AoSMC*